

1 **Title: Chronic *Salmonella* Infection Contributes to Gallbladder Carcinogenesis**

2 **Authors:** Agila Kumari Pragasam<sup>1#</sup>, Sonalika Maurya<sup>2#</sup>, Kajal Jain<sup>3#</sup>, Sujoy Pal<sup>4</sup>, Christu Raja<sup>4</sup>, Shakti  
3 Kumar<sup>1</sup>, Ayushi Purohit<sup>1</sup>, Dibyabhaba Pradhan<sup>4</sup>, Kirti Kajal<sup>2</sup>, Daizee Talukdar<sup>1</sup>, Anand Narayan Singh<sup>4</sup>, Jyoti  
4 Verma<sup>1</sup>, Pradipta Jana<sup>1</sup>, Shaifali Rawat<sup>5</sup>, Pallavi Kshetrapal<sup>6</sup>, Asuri Krishna<sup>3</sup>, Subodh Kumar<sup>7</sup>, Virinder Kumar  
5 Bansal<sup>3</sup>, Rajni Yadav, Bhabatosh Das<sup>1\*8</sup>, Chittur V Srikanth<sup>2\*8</sup>, Pramod Kumar Garg<sup>4\*9</sup>

6  
7  
8 **Author's affiliations:**

9 *1-Infection and Immunology Division, Translational Health Science and Technology Institute, Faridabad, India*

10 *2-Laboratory of Gut Infection and Inflammation Biology, Regional Centre for Biotechnology, Faridabad, India*

11 *3-Department of Pediatrics, All India Institute of Medical Sciences, New Delhi*

12 *4-Department of Gastroenterology and Human Nutrition, All India Institute of Medical Sciences, New Delhi,*  
13 *India*

14 *5-Department of Pathology, All India Institute of Medical Sciences, New Delhi, India*

15 *6-Pediatric Biology Center, Translational Health Science and Technology Institute, NCR Biotech Science*  
16 *Cluster, Faridabad, India*

17 *7-Department of Surgery, All India Institute of Medical Sciences, New Delhi, India*

18  
19 **Footnotes:**

20 *# Equal contribution*

21 *8 Senior authors with equal contribution*

22 *9 Lead author*

23 *\*Corresponding authors*

24  
25 **Contact info:**

26 **Pramod Kumar Garg:** *Department of Gastroenterology and Human Nutrition, All India Institute of Medical*  
27 *Sciences, New Delhi -110029, India. Email: pgarg10@gmail.com*

28 **Chittur V Srikanth:** *Laboratory of Gut Infection and Inflammation Biology, Regional Centre for*  
29 *Biotechnology, Faridabad – 121001, India. Email: cvsrikanth@rcb.res.in*

30 **Bhabatosh Das:** *Functional Genomics Laboratory, Centre for Microbial Research, Infection and Immunology*  
31 *Division, Translational Health Science and Technology Institute, NCR Biotech Science Cluster, 3rd Milestone,*  
32 *Faridabad – Gurgaon Expressway, PO box 04, Faridabad – 121001, Haryana, India. Phone: +91-129-*  
33 *2876471; Fax: 0129-2876500; Email: [bhabatosh@thsti.res.in](mailto:bhabatosh@thsti.res.in)*

38 **Summary:**

39 Gallbladder cancer (GBC) is an aggressive gastrointestinal cancer. Gallbladder stones and  
40 chronic microbial infections though implicated in its carcinogenesis are not proven risk  
41 factors and the underlying mechanisms are largely unknown. Here, we show an increased  
42 abundance of *Salmonella* in the gut microbiome of patients with GBC and culturable  
43 *Salmonella* Typhimurium from their GBC tissue. Comparative genomics of *S. Typhimurium*  
44 isolated from GBC tissue showed a high invasive index. *S. Typhimurium* isolates harbored  
45 horizontally acquired potential virulence functions in their accessory genome. Chronic *S.*  
46 *Typhimurium* infection displayed inflammation, pre-neoplastic changes and tumor promoting  
47 mechanisms in a mouse model with gallbladder stones, including activation of the epigenetic  
48 modulator Kdm6b. Inhibition of Kdm6B reduced tumor size in NOZ cells engrafted in SCID-  
49 mice. Transcriptomic analysis of human GBC tissue supported the proposed  
50 mechanisms. Thus, we show a causal association between GBC and chronic *Salmonella*  
51 infection and a host epigenetic mechanism in gallbladder carcinogenesis.

52  
53 **Keywords:** Gallbladder cancer, Gallstones, *Salmonella*, Microbiome, Infection, Inflammation,

54  
55  
56  
57  
58  
59  
60  
61  
62  
63  
64

65 **Introduction:**

66 Gallbladder cancer (GBC) is one of the most lethal cancers with a 5-year stage-independent  
67 survival rate of 20% and overall mean survival of <6 months (Shaffer & Hundal, 2014). The  
68 dismal prognosis is due to aggressive biological behavior of the tumor and the delay in diagnosis  
69 (Batra et al., 2005). Even in the United States, <20% of GBC are diagnosed in the early stages.  
70 Curative surgery is possible in only 10-20% of patients and the response to chemoradiotherapy is  
71 also poor (Sharma et al., 2010). The incidence of GBC is high in many parts of the world such as  
72 Chile, Mexico, Bolivia, India, non-Hispanic blacks in the US, around the Mediterranean and  
73 Japan (Sharma et al., 2017). For example, the incidence of GBC was reported to be 12.3/100,000  
74 for males and 27.3/100,000 for females in Chile (Shaffer & Hundal, 2014) necessitating the need  
75 for population based preventive strategies.

76 Although various risk factors for GBC have been reported, a definite causal association with a  
77 particular risk factor has not yet been established. The most likely causal association has been  
78 with gallbladder stones since 60-90% of patients with GBC have associated gallbladder stones  
79 (Bolyen et al., 2019; Bruno et al., 2009). Cohort studies in patients with gallstones have also  
80 suggested an increased risk of GBC (Attili et al., 1995). Patients with gallstones have been  
81 shown to develop pre-neoplastic lesions in the gallbladder mucosa. In a study of 350 patients  
82 with gallbladder stones, we have shown that there was sequential occurrence of one or more  
83 preneoplastic lesions in the gallbladder in 64% of patients – hyperplasia in 32%, metaplasia in  
84 47.8%, dysplasia in 15.7%, and carcinoma in situ in 0.6% (Jain et al., 2014). In addition, we  
85 found accumulation of loss of heterozygosity (LOH) in *p53*, *p16*, *DCC*, and *APC* genes in those  
86 pre-neoplastic lesions. However, despite evidence of a strong association of gallstones with  
87 GBC, contrast between countries with a high and low prevalence of gallstones, and incidence of  
88 GBC questions the causal association of gallstones as a single risk factor for GBC. For example,  
89 10-15% of the US adult population have gallbladder stones but the overall incidence of GBC is  
90 much lower i.e. 1.3/100,000 (Everhart & Ruhl, 2009; Stinton & Shaffer, 2012). On the other  
91 hand, the prevalence of gallstones is lower at 4.1% in India but the age standardized incidence of  
92 GBC is much higher at 11.8/100,000 population (National Cancer registry programme 2012-  
93 2014) (Horesh et al., 2021). These observations suggest additional risk factor(s) in the  
94 etiopathogenesis of GBC. Chronic gallbladder infection has long been suspected to be an  
95 important risk factor for GBC. In a case-control study, we had shown that chronic typhoid carrier  
96 state was associated with GBC (Odds Ratio = 14; 95% CI 2-92). A meta-analysis of >1000  
97 cases of GBC has shown that the relative risk was 4.6 (95% CI: 3.1-6.8) for anti-*Salmonella* Vi  
98 antibody and 5.0 (95% CI: 2.7-9.3) for bile or stool culture positivity for *Salmonella* infection

99 (Koshiol et al., 2016). *Salmonella* is transmitted by the feco-oral route which is facilitated by  
100 poor hygiene, and food and water contamination – conditions prevalent in areas with a high  
101 incidence of GBC (Jain et al., 2013). Gut microbiota derived toxins and metabolites have been  
102 implicated in carcinogenesis of some cancers (Rowland, 2000). However, the role of a particular  
103 chronic bacterial infection in the carcinogenesis of GBC and mechanism(s) thereof are not well  
104 known. In the present communication, we report results of: (1) human studies to examine (a)  
105 alteration in gut microbiome in patients with GBC (b) demonstration of viable *Salmonella* in the  
106 gallbladder tissue of patients with GBC, (c) virulence and invasive factors of the isolated  
107 *Salmonella* in patients with GBC and (d) genome-wide expression in GBC tissue to understand  
108 the mechanistic pathway(s) in its carcinogenesis, and (2) experimental studies to show (a) the  
109 role of enteric *Salmonella* infection and gallstones in the carcinogenesis of GBC in a murine  
110 model, and (b) the epigenetic alterations in the pathogenesis of GBC.

111

## 112 **Results:**

113 **Composition of gut microbiota in patients with gallbladder cancer is altered and is**  
114 **enriched with *Salmonella* and other proteobacteria:** In a case-control study, we investigated  
115 the fecal microbiome in 20 GBC patients and 20 patients with gallbladder stones (GS) and  
116 compared it with previously reported 50 healthy adult Indians living in the same geographical  
117 area (Das et al., 2018). Demographic details of patients are provided in **Suppl. Table S1**. The  
118 community microbial DNA extracted from fecal samples generated a total of 17,52,338 raw  
119 reads and 17,17,739 processed reads (post quality filtering and de-multiplexing), with an average  
120 44,459 reads per subject (average varying between 72889 and 22719 reads across the samples).  
121 The average read length obtained was 1306 bps, which covers all the variable regions of the 16S  
122 rRNA gene (read averages ranged from 972 to 1366 bps) (**Table 1, Suppl. Table S2**). Our  
123 analysis showed that the composition and relative abundance of *Actinobacteriota*, *Bacteroidota*,  
124 *Cyanobacteria*, *Spirochaetota*, and *Verucomicrobiota* were similar in the fecal samples of GBC  
125 and GS patients and healthy subjects (**Figure 1; Suppl. Table S2**). However, the relative  
126 abundance of three bacterial phyla viz. *Proteobacteria*, *Acidobacteria*, and *Tenericutes* was  
127 significantly higher in the GBC and GS patients compared to the healthy subjects (**Figure 1**).  
128 Furthermore, we observed distinct interquartile range (IQR) of relative abundance distribution in  
129 *Proteobacteria* ( $IQR_{GBC} = 0.0232$ ,  $IQR_{GS} = 0.0122$ ), *Acidobacteriota* ( $IQR_{GBC} = 0.0126$ ,  $IQR_{GS}$   
130  $= 0.00904$ ), and *Tenericutes* ( $IQR_{GBC} = 0.00899$ ,  $IQR_{GS} = 0.00621$ ) in the fecal samples of GBC  
131 and GS patients compared to the healthy subjects. Among all three phyla, the IQR of relative  
132 abundance of the phylum *Proteobacteria* was considerably higher in the GBC group (**Figure 1**).

133 The composition of the fecal microbiota was further examined at the levels of class, order, genus  
134 and species. The sequencing depth employed here revealed a total of 1001 bacterial genera and  
135 505 different species in all the GBC and GS patients. On analyzing the alpha diversity of the  
136 fecal microbiota of GBC, GS patients and healthy subjects, we found that there was a significant  
137 difference in the Chao index (Kruskal Wallis H test, P value =5.5e-0.8), whereas no difference  
138 was observed in Shannon and Simpson diversity indices (**Suppl. Figure S1; Suppl. Table S3**).  
139 To identify disease specific microbial taxa, we considered the differences in relative abundance  
140 of bacterial taxa. At the genus level, we observed that 29 genera were differently abundant across  
141 the three groups (one-way ANNOVA at P-value<0.05). The relative abundance of *Salmonella*,  
142 was higher in GBC compared to GS patients. The highest abundance of *Salmonella* observed in a  
143 GBS patient was 0. 0226. Interestingly, *Salmonella* was absent in the fecal sample of any healthy  
144 subjects. The genus *Streptococcus* was significantly high (Kruskal Wallis H test, P-value<0.05)  
145 in the GBC patients compared to the GS and healthy subjects **Suppl. Figure S2**. However, a few  
146 of the healthy samples were also found to have *Streptococcus* in their fecal samples. The  
147 *Prevotella pallens* had lower abundance in GBC patients as compared to GS, whereas it was not  
148 detected in the healthy subjects. We also observed that 7 bacterial genera belonging to  
149 *Proteobacteria* had significantly different abundance patterns across the three groups (Kruskal  
150 Wallis H test, P-value<0.05) **Suppl. Figure S2**. *Salmonella* (p-value:  $5.22 \times 10^{-18}$ ), *Burkholderia*  
151 (p-value:  $5.137 \times 10^{-18}$ ), *Serratia* (p-value:  $5.250 \times 10^{-18}$ ), *Acinetobacter* (p-value:  $3.306 \times 10^{-14}$ ),  
152 *Klebsiella* (p-value:  $1.34 \times 10^{-8}$ ), *Pseudomonas* (p-value:  $2.01 \times 10^{-7}$ ) and *Haemophilus* (p-value:  
153  $2.11 \times 10^{-6}$ ), were observed to have the higher abundance in GBC and GS patients as compared to  
154 the healthy subjects (**Suppl. Figure S2; Suppl. Table S4**). The relative abundance of  
155 *Salmonella*, *Burkholderia* and *Serratia* was higher in GBC compared to GS patients.  
156 Furthermore, the genera *Salmonella*, *Serratia* and *Burkholderia* were absent in healthy subjects.

157

#### 158 **Culture independent analysis of microbial composition in the GBC tissue:**

159 Since we observed that the relative abundance of *Salmonella* in the gut microbiota of GBC  
160 patients was very high compared to the other two groups, we studied if *Salmonella*, being  
161 invasive in nature with an ability to survive in bile, was present in the GB cancer tissue. We  
162 tested the microbiota composition of surgically resected gallbladder cancer tissue from the GBC  
163 patients (n=17). Of these 17 samples, we could amplify the 16S rRNA region of the bacteria in 9  
164 samples. After quality filtration ~72% to 76% paired reads of 16S rRNA gene derived from the  
165 gallbladder tissue were subsisted for taxonomic assignment (**Suppl. Table S2**). About 26% to  
166 34% quality filtered paired reads with average of ~435-bp read lengths were used as input to the

167 QIIME2 program to generate the OTU table. The OTUs rarefaction curve showed very less  
168 microbial diversity and around 30 OTUs were identified (**Suppl. Figure S3**) which suggested  
169 that the gallbladder might not be a conducive residence and could provide a niche environment  
170 for only a few microbial species. The identified 30 OTUs belonged to 7 phyla in which  
171 *Proteobacteria* was the most dominant (**Suppl. Figure S4**). The numbers of reads of the  
172 remaining phyla were too less that they could be considered as a rare phylum of the ecological  
173 niche. At the genus level, *Salmonella* was the most dominant bacterium across all 9 samples  
174 (**Suppl. Figure S5**). Apart from *Salmonella*, four other bacterial genera namely *Pseudomonas*,  
175 *Burkholderia*, *Klebsiella*, and *Ralstonia* were also observed in most of the gallbladder tissue  
176 samples with similar abundances.

177  
178 **Insights into genomic potency and functionality of *Salmonella* residing in the gallbladder**  
179 **tissue of GBC patients:**

180 Since *Salmonella* was the most abundant bacterial genus and distributed in all 9 GBC tissue  
181 samples, we isolated the bacterium for exploring its genomic repertoires, and genetic potential  
182 with regard to virulence and disease pathogenesis. The characterization of the taxonomy of the  
183 isolate by complete 16S rRNA gene sequencing revealed it to be *Salmonella enterica* var  
184 Typhimurium. Whole genome shotgun sequencing of 28 *Salmonella* Typhimurium isolates was  
185 performed. A total of 11974408 paired-end (PE) reads (~6.71GB data) with 280 bp mean read  
186 length were generated. Of these reads, 11862942 (~6.64 GB data) had Phred Quality Score  
187 (Q) >20 and were used by SPAdes to generate 11x to 43x genome coverage (**Suppl. Table S5.1**).  
188 RAST annotation details are mentioned in **Suppl. Table S5.2**.

189 Genomic potency and diversity of the *S. Typhimurium* were determined based on the MLST  
190 sequence types (ST) and also by whole genome SNP analysis. Among the study isolates, 23/28  
191 were identified as ST19, while 5 genomes were of unknown STs due to one or two missing  
192 genes in the draft assemblies. However, the available allelic profiles of 5/7 genes were found  
193 similar to ST19 and thus we predicted these genomes belonged to clonal complex ST19 (CC19)  
194 (**Table 3**). Further, whole genome SNP based phylogenetic analysis of *S. Typhimurium* was  
195 performed along with the previously published genomes belonging to ST19, in comparison to the  
196 other most common STs of ST34 and ST313 collected across the globe ( $n=2490$ ) (**Suppl. Table**  
197 **S6**). Majority of these were sourced from fecal samples, except the African strains of invasive  
198 ST313. The phylogenetic positioning of *S. Typhimurium* was characterized in regards to their  
199 STs and spatiotemporal profile. The GBC sourced isolates in the present study clustered within

200 the ST19 genomes (**Figure 2a**). Notably, within the ST19 group, the contemporary GBC isolates  
201 formed a distinct sub-cluster along with 12 other genomes from North America and Europe  
202 sourced from fecal samples during the period 2006 to 2020 (**Figure 2a**). Five isolates that were  
203 not genotyped by MLST also clustered within the study isolates of ST19, confirming these  
204 genomes as ST19/CC19.

### 205 **Invasive index of ST19 *S. Typhimurium* isolated from the GBC tissue**

206 The potential invasiveness of each of the GBC sourced ST19 *S. Typhimurium* isolates was  
207 investigated against the genome degradation event captured with the pre-defined 196 genes. The  
208 GBC isolates displayed an invasiveness index score of predominantly  $>0.0823$  (except for a  
209 few), which was slightly higher than reference *S. Typhimurium* LT2 (0.0823) (**Figure 3a**).  
210 Minor differences in the score could be due to the limited genome degradation events with a few  
211 genes out of the 196 genes in the GBC isolates as compared to the African invasive ST313. Of  
212 note, 1/3<sup>rd</sup> of isolates from each patient displayed a higher invasive score compared to the other  
213 isolates sourced from the same patient, indicating heterogeneity and the likelihood of within-host  
214 evolution of *S. Typhimurium*. On comparison, we found that the isolates with a high mutation  
215 frequency displayed a high invasive index score (except for P7B, P8B and P9B) (**Figure 3b**).  
216 Thus, the overall observed signatures of gene degradation events led to the increased invasive  
217 potential of this pathogen in GBC than the non-invasive ST19 strains.

218 As the invasive isolates in the present study were sourced from GBC, the dynamics of  
219 pseudogenization/gene degradation that favored the invasiveness were examined to identify host  
220 adaptation signatures in comparison with the African invasive ST313. This phenomenon of  
221 hypothetically disturbed coding sequences (HDCS)/pseudogenes has been characterized by the  
222 presence of multiple mutations and was captured in the GBC isolates mapped against the  
223 reference genome *S. Typhimurium* LT2. Firstly, all the genomes displayed a notable 10 bp  
224 nucleotide deletion in GBC ST19 isolates causing a frameshift mutation in the virulence gene  
225 *lpfD*. This encodes for a long polar fimbriae that helps colonize the Peyer's patches but its  
226 inactivation due to frameshift prevents the pathogen's interaction with M-cells. Further, in the  
227 mutational profiling, missense mutations were the most abundant that ranged from 193 to 261  
228 mutations among all GBC *S. Typhimurium* isolates (**Figure 3b**). In addition, 11 frameshift  
229 mutations were found to be common in all the 28 genomes, while a few genomes harbored  
230 additional mutations that ranged from 11 to 18. The mutation profile was compared with the top  
231 10 invasive ST313 signatures to infer the invasiveness potential of the GBC isolates **Suppl.**  
232 **Figure S6a**. First notable signature, a one-bp deletion in the *ratB* gene (STM2514: 5807delT),  
233 resulted in the frameshift of the protein at position 1936/2435, thereby forming a pseudogene.

234 Second was the missense mutation in the *sseI* gene encoding for Gifsy-2 prophage putative type  
235 III secreted protein (STM1051: T308C) which led to the amino acid change of Asp103Gly  
236 (D103G), making this as a non-functional protein. Third was the inactivation of a virulence gene  
237 *avrA* (one nucleotide deletion 799A), an effector protein that inhibits the NFκB signalling  
238 pathway. Its non-functionality hinders with the modulating ability of the pro-inflammatory  
239 response during an infection. These three key signature changes might have favored the ST19 *S.*  
240 Typhimurium in crossing the intestinal barrier to become invasive. Further, 18 genes with  
241 missense mutations that were predefined as pseudogenes in the ST313 population were also  
242 found in ST19 GBC isolates. Eleven other frameshift mutations were also identified besides  
243 ST313 signatures. Moreover, the differences in the mutational profile (missense) within the 28  
244 study isolates were observed with 3 strains each from 8 patients and 2 strains each from 2  
245 patients, respectively **Suppl. Figure S6b**. Such heterogeneity in the mutational patterns within  
246 the same patient is remarkable and is being documented for the first time.

247

#### 248 ***S.* Typhimurium isolated from the GBC harbored distinct accessory genomes containing** 249 **potential virulence functions:**

250 A comparative pan genome analysis was carried out to analyze the differences in the genome  
251 composition of different STs such as ST19, ST34 and ST313. Among the 2518 genomes, we  
252 identified 13,750 as total gene families. The number of core genes (99 to 100%) was 3822, soft-  
253 core genes (95 to 99%) were 185, shell genes (15 to 95%) were 1123, and cloud genes were  
254 8620 (0 to 15%). The phylogenetic tree with the clades of each represented STs showed similar  
255 gene content profiles. However, regions/genes that were likely to be shared by the specific STs  
256 were highlighted as shown in the Phandango illustration (**Figure 4**). These main differences  
257 were in the accessory genome content with the presence of prophage elements that were also ST  
258 specific. **Figure 4a-d** shows the complete pan genome profile of the *S.* Typhimurium with  
259 respect to different STs and their associated metadata.

260 Putative virulence factors screened by the VFDB analyser tool identified 11 virulence factor  
261 classes corresponding to 160 virulence factor genes in the study isolates. The candidate virulence  
262 factors are associated with secretion systems which include TTSS (SPI01encode), TTSS  
263 (SPI02encode), TTSS effectors translocated via both systems, TTSS01 translocated effectors and  
264 TTSS02 translocated effectors. Additionally, VF class like fimbrial adherence determinants (*csg*,  
265 *bcf*, *fim*, *lpf*, *pef*, *saf*, *stb*, *stc*, *std*, *stf*, *sti*, *stj*) macrophage inducible genes (*mig-14*, *mig-5*),  
266 magnesium uptake (Mg<sup>2+</sup> transport), non fimbrial adherence determinants (*misL*, *ratB*, *shdA*,  
267 *sinH*), serum resistance (*rck*), and stress adaptation (*sodCI*) genes were also identified in the



268 GBC isolates . The different VF classes along with their corresponding VF genes found in the  
269 present study isolates are illustrated in **Suppl. Figure S7**.

270 Three important proinflammatory SPI-1-T3SS effector proteins *sopE2*, *sopB/sigD* and *sopA* were  
271 found in all 28 isolates. In contrast, one of the T3SS effector protein *sopD* was present in 22/28  
272 (78.5%) genomes. Virulence factor genes with anti-inflammatory properties, *gogB*, *gogA*, *SseK1*,  
273 *SseK2*, *SopA*, *SopB/sigD*, *sspH2* were identified in all the 28 genomes whereas *sptP* and *spvC*  
274 were identified in 11/28 (39%) and 12/28(42%) genomes respectively. Other effector proteins  
275 like, *spvD*, *spvC* and *avrA* which directly target inflammatory signalling in a negative way were  
276 also found to be present in the GBC *Salmonella* isolates. Of these, *spvD*, which is involved in  
277 inhibiting NF- $\kappa$ B (Rolhion et al., 2016) was identified only in 2 (0.7%) genomes (P5C and P6B).  
278 *sodCl* which corresponds to stress adaptation was found to be present in 96% (27/28) of  
279 genomes. The presence and absence of these pro-inflammatory and anti-inflammatory virulence  
280 genes in the GBC isolates are depicted in **Suppl. Figure S8**. From our analysis, we found that  
281 the same virulence profile was seen in the isolates from four patients whereas there was  
282 heterogeneity in the distribution of virulence genes in isolates from five patients.

283

#### 284 **Horizontally acquired plasmids and prophages with virulence potency in the genome of *S.*** 285 ***Typhimurium* isolated from the GBC tissue:**

286 Plasmids harboring virulence genes are of special importance since they are involved in the  
287 dissemination of antibiotic resistance. PLSDB identified four circular plasmids in the GBC  
288 *Salmonella* isolates (**Table 4**). First was a 69.65 Kb *S. Typhimurium* strain AUSMDU00027951  
289 plasmid P02 (NZ\_OU015330.1) with a GC content of 52.67% in 28 sequenced genomes. Second  
290 was a 147Kb *Salmonella enterica* subsp. Senftenberg strain NCTC10384 plasmid 3  
291 (NZ\_LN868945.1) has a similar GC% as the previous plasmid in 15 of the 28 (53%) genomes.  
292 Both these plasmids harbor *entD*, which encodes phosphopantetheinyl transferase component of  
293 enterobactin synthase multienzyme complex (Enterobactin) as the virulence factor. Third  
294 plasmid was a *Salmonella enterica* subsp Enteritidis strain 81-1705 plasmid pSE81-1705-3  
295 (NZ\_CP018654.1) of 33Kb in 96% (27/28) of the genomes of *S. Typhimurium*, which harbored  
296 *galU*, a glucosephosphate uridyl transferase gene involved in immune modulation. The fourth  
297 plasmid was present in 39% of the GBC isolates. This plasmid carries 5 virulence genes (*pefC*,  
298 *spvB*, *spvC*, *rck*, *pefB*). Besides, 2 plasmid replicons having a capacity to activate and control  
299 replication (*InCFII* and *InCFI*) were also identified within this plasmid. On basic local alignment  
300 search tool BLASTn analysis, we found that *Salmonella enterica* subsp. CFSAN002003 plasmid  
301 showed identity and coverage of 99.99% with the virulence plasmid of *S. Typhimurium* LT2

302 (pSLT ) which is of 94Kb. pSLT has an 8Kb region which encodes the virulence gene *spv* which  
303 has been reported to increase the bacterial growth rate at the time of the systemic phase of the  
304 disease progression (Hiley et al., 2019). Heterogenicity was observed in 60% of the patients  
305 whereas in only 40% of the patients there was similarity within the isolates. BLASTn results  
306 further confirmed the presence of these four plasmids within the GBC isolates having query  
307 coverage of >90 and percent identity of >98%.

308 Three lysogenic prophages were initially identified by the Phage search tool enhanced release  
309 PHASTER in the annotated genome of *S. Typhimurium*. Gifsy-1, Gifsy-2 and  
310 salmon118970\_sal3 were commonly present in all the 28 *S. Typhimurium* isolates.  
311 Salmon118970\_sal3 possesses one virulence gene (*SseK2*). Gifsy-1 (encoding *gogA* and *gogB*)  
312 and Gifsy-2 (encoding *sodCl* and *ssel*) along with four phage remnants Def1-4 having virulence  
313 genes were also identified in the genome of ST313 representative strain D23580 which has been  
314 reported to cause invasive disease in sub-Saharan Africa (Kingsley et al., 2009). We then did a  
315 manual BLASTn analysis to confirm the invasiveness in our studied GBC isolates against *S.*  
316 *Typhimurium* D23580 genome as a reference. Results indicated that Def-2 encoding *sopE2* as  
317 the virulence gene was found in all the 28 genomes. Def-1 was also found to be present in the  
318 three of the genomes with a query coverage of less than <35%. Three GBC genomes of *S.*  
319 *Typhimurium* were found to possess Def-3 remnants having an anti-inflammatory virulence  
320 gene *sspH2* with less query coverage in comparison to the other isolates. A 20Kb region (*gtrBb*)  
321 from the Def-4 phage encoding virulence trait was identified in 25 GBC isolates. ST64B  
322 prophage with the virulence gene *SseK3* was identified in all 28 isolates. The overall profile for  
323 the phage analysis within the isolates was found to be similar. The presence and absence of  
324 prophage and prophage remnants in the GBC isolates in comparison to D23580 are mentioned in  
325 Table 5.

326

### 327 **Enteric *Salmonella* chronically colonizes Gallbladder in a Gallstone mice model**

328 To examine the role of chronic *Salmonella* infection in the pathogenesis of GBC, we  
329 developed a modified version of a mice model of gallstone disease along with chronic  
330 *Salmonella* infection following a previously published protocol (Crawford et al. 2010). Our  
331 methodology involved four weeks old wild type FVB mice (4-6 animals per cohort) fed with  
332 mouse chow supplemented with 1% cholesterol and 0.5% cholic acid for 9 weeks. As shown  
333 in **Figure 5**, lithogenic diet feeding led to development of gallstones in these mice (hereafter  
334 referred as Lithogenic Diet or LD group). A subset of gallstone mice was infected with  
335 *Salmonella typhimurium* (strain SL3261) by oral gavage (referred to as Lithogenic diet + ST

336 group or LDST). The SL3261 is an attenuated *Salmonella* strain bearing an *aroA* deletion  
337 well suited for chronic infection in mice (Eisele NA et. al. 2013). Separate groups of mice fed  
338 with a regular diet and mock-infected (Control) or those fed with a regular diet but infected  
339 with SL3261 (Control ST) were also included in the study.

340 Gallstone developed in 100% of the lithogenic diet fed animals. The stones were multiple  
341 with a range of different colors including dark green, red (in LD-ST group) and pale yellow  
342 (in the LD group). The size of the stones ranged approximately between 0.1-0.5mm in  
343 diameter (**Figure 5b**). Mice infected with *Salmonella* also developed splenomegaly (**Figure**  
344 **5c**). In these mice (LD group and LD-ST group), the liver was enlarged with a change in  
345 color to pale red possibly due to diet induced accumulation of fat (LD group and LD-ST  
346 group), while the control mice did not show any of these phenotypes (**Figure 5c**). Notably,  
347 the LD-ST group mice showed the presence of *Salmonella* in internal organs, 15 days post  
348 infection, as revealed by colony forming units (cfu) of *Salmonella* in the liver (**Suppl. Figure**  
349 **S9**), and the portion of the common bile duct connected to the gallbladder. The presence of  
350 *Salmonella* was further confirmed by 16S qRT-PCR assay and electrophoresis of the  
351 amplicons on 1.5% agarose gel (**Figure 5d**). *Salmonella* fecal shedding was also seen by the  
352 presence of its colony forming units (cfu) in the MacConkey agar plates and further  
353 confirmed by qRT-PCR assay and agarose gel electrophoresis. (**Figure 5e**). Together these  
354 data revealed the successful development of a gallstone-mice model with chronic *Salmonella*  
355 infection.

### 356 **Chronic Salmonella infection and gallstone disease cause chronic inflammation and** 357 **induce pre-malignant changes in the gallbladder mucosa**

358 The histology of the gallbladder tissue sections was analysed. As anticipated, the control  
359 group showed healthy normal tissue histology (**Figure 6a**). However, signs of inflammation  
360 marked by infiltration of immunocytes neutrophils were seen in the LD-group, ST-group and  
361 in LD-ST mice. Importantly, pre-malignant changes in the form of hyperplasia and  
362 metaplasia developed only in the LD-ST group at 4 months post infection (**Figure 6a**). These  
363 changes were also evident in the histopathology scoring (**Figure 6a** right panel). These pre-  
364 malignant changes were not evident at 15 days post infection in these groups. At later stages  
365 of infection (i.e. 8.5 month post infection), more severe changes such as thickening of the  
366 gallbladder wall, fibrosis, hyperplasia and metaplasia were evident in the LD-ST group  
367 (**Figure 6c**). The pathological scores indicated that wall thickening and hyperplasia were  
368 maximum in LD-ST group followed by Control-ST mice. Taken together, these data led us to  
369 conclude that gallstone along with chronic *Salmonella* infection caused chronic inflammation

370 and induced pre-malignant changes in the gallbladder tissue. Mucins are a critical  
371 determinant of the nature of a tissue and are often used as an indicator of different  
372 pathological conditions. Neutral mucins are present in healthy gallbladder tissue epithelium,  
373 whereas acidic mucins are present in metaplasia associated gallbladder tissues. Therefore, we  
374 carried out AB-PAS staining to examine the type of mucins in the different groups of mice.  
375 The gallbladder tissue sections of 4 months infected LD-ST group and LD-group mice  
376 showed multiple zones of deep blue staining which indicated the presence of acidic mucins  
377 (**Figure 6c**). In contrast, the control and Control-ST group showed normal neutral mucins.  
378 These results are indicative of significant mucosal changes in the LD-ST mice (**Figure 6c**).

379

### 380 **Chronic Salmonella infection induces epigenetic changes involving Kdm6B in the** 381 **murine gallbladder**

382 We recently reported the involvement of Kdm6B, a histone demethylase, to be necessary for  
383 chronic *Salmonella* infection (Rana et al., 2021). In this report, up regulation of Kdm6B  
384 expression was shown to reprogram infected macrophages into non-bactericidal M2 like  
385 spectrum (Rana et al., 2021). The presence of pre-malignant changes in the LD-ST mice  
386 tissue sections described above prompted us to investigate possible involvement of epigenetic  
387 alterations. We examined the status of Kdm6B in the *Salmonella* infected gallstone-mice. We  
388 found that the expression of epigenetic modulator Kdm6B was upregulated at the mRNA  
389 level in LD-ST mice compared to the other groups (**Suppl. Figure S10a**). At the protein level  
390 as well, Kdm6B expression was higher in *Salmonella* infected mice (**Figure 7a-b**) at 5 month  
391 post infection. To see the effect of infection in longer durations, we allowed infection to  
392 proceed for 1.8 years. The increase in Kdm6B was dramatic in LD-ST mice (2 out of 4 mice)  
393 at 1.8 years (**Figure 7b**). Taken together, these results suggest that chronic *Salmonella*  
394 infection alone increased Kdm6B expression but along with presence of gallstones led to  
395 further increase in the Kdm6B expression which could contribute to the formation of pre-  
396 malignant lesions.

397 Therefore, we examined if *Salmonella* induced Kdm6B upregulation may be contributing to  
398 activation of genes favoring tumorigenesis. A decreased expression of tumor suppressor  
399 genes p16 and p53 was observed in Control-ST and LD-ST group compared to the control  
400 group and LD group. p16 showed significant ~5-fold downregulation in all the 3 groups (LD  
401 group, ST group and LD-ST group mice) compared to uninfected control of 8.5 months batch  
402 (**Figure 7c-d**). p53 was also drastically downregulated in gallbladders of LD, LD-ST and  
403 Control-ST group but not in untreated control group of mice of 8.5 months post infection.

404 Notably, among these groups, ST mice showed 13-fold downregulation compared to  
405 Gallstone-ST, which showed 10-fold decrease in expression (**Suppl. Figure S10**). These data  
406 indicate pro-tumorigenic molecular alterations occurring in gallbladder tissue of Gallstone-  
407 ST and ST mice.

#### 408 **Kdm6B in Human GBC:**

409 The status of Kdm6B in human gallbladder cancer tissue was examined by immunoblotting  
410 from lysates of patient biopsy samples (**Figure 7e**). A significant increase in Kdm6B  
411 expression in GBC samples compared to those from gallstone or non-malignant patient  
412 controls was observed. In the case of gallstone samples, only a slight upregulation of the  
413 expression of Kdm6B was seen.

#### 414 **Genome-wide expression profiling of human gallbladder cancer to understand the** 415 **pathways involved in GBC:**

416 Genome-wide expression profiling was done in the gallbladder tissue samples collected from 16  
417 GBC patients and 16 gallstones controls (matched for age and sex) that underwent  
418 cholecystectomy. All 16 were adenocarcinoma on histology. The age and sex distribution of the  
419 patients and controls are provided in **Suppl. Table S7**.

420

#### 421 **Differentially expressed genes on mRNA profiling:**

422 To identify DEGs associated with GBC, expression profiles of 32 human samples including 16  
423 adenocarcinoma patients and 16 samples from gallstone disease controls were analyzed using  
424 LIMMA. The criteria of  $FC \geq 1.5$  for up-regulated and  $FC < 1.5$  for down-regulated with  $\leq 0.05$   
425 were used to identify the significant DEGs. The total number of differentially expressed  
426 transcripts was 480 that had significant p-value and adjusted p-value (**Figure 8**). Overall, 340  
427 genes could be annotated from 480 transcripts (205 upregulated and 135 downregulated). The  
428 human transcriptomics data suggested that several genes including ADAMTSL5, CX3CR1,  
429 HMGA2, MMP7, EPHB2, TYMP, HLA-A, MK167, and HDGF were differentially regulated in  
430 GBC tissue as compared to those with gallstones. The list of differentially expressed genes is  
431 given in **Suppl. Table S7**. Functional analysis through KEGG (Kyoto Encyclopaedia of Genes  
432 and Genomes) showed that differentially expressed genes were related to metabolic pathways,  
433 neutrophil extracellular trap formation, alcoholism and transcriptional mis-regulation in cancer  
434 (**Figure 8**). A few of the dysregulated genes mentioned above identified through human  
435 transcriptome data were further tested experimentally in the context of *Salmonella* infection.

436

### 437 **Experimental evidence of the role of Kdm6B:**

438 The expression of genes, which were identified by GBC tissue transcriptomics, was examined  
439 in NOZ cells, a cell line derived from human gallbladder carcinoma tissue. NOZ were  
440 cultured and either sham infected or infected with *Salmonella* for 1 hr. Among these genes,  
441 those with regulatory function, such as- ADAMTSL5 (maintains oncogenic signaling, master  
442 regulator of carcinogenesis), CX3CR1(C-X3-C motif chemokine receptor 1, known for cell  
443 migration and tumor invasion) and SPSB4 (regulator of protein ubiquitylation, plays a role in  
444 cell invasion) were significantly dysregulated (**Figure 7f**). We next examined if Kdm6B  
445 function was required for the upregulation of these genes by carrying out chromatin  
446 immunoprecipitation. A 3-fold higher binding of Kdm6B in the promoter of ADAMTSL5  
447 was seen in NOZ cells infected with *Salmonella* compared to control cells (**Figure 7g**). In  
448 line with this we also observed a significant decrease in H3K27me3 mark, i.e. histone-3  
449 lysine 27 tri-methylation (**Figure 7h**). Based on background literature and these findings, we  
450 hypothesized that *Salmonella* in the gallbladder causes epigenetic alterations to drive  
451 tumorigenesis.

452 Furthermore, infection of NOZ cells resulted in an increase in expression of Kdm6B at 4, 7  
453 and 18 hrs post infection (**Suppl. Figure S11a**). Tumour suppressor gene p53 was also found  
454 to be downregulated during infection in a time dependent manner (**Suppl. Figure S11b**).  
455 *Salmonella* specific inflammatory markers IL8 and IL1 $\beta$  were also found to be upregulated.  
456 Moreover, expression of IL-8 was increased early during infection i.e. 4 hrs, while IL-1 $\beta$  at  
457 later stage of 18 hrs post infection. The protein levels of Kdm6B showed an increase at 4 and  
458 8 hrs post infection in these cells (**Suppl. Figure S11c**). To further understand the underlying  
459 mechanism, we cultured primary gallbladder epithelial cells from mice gallbladder followed  
460 by infecting them with mCherry-labeled *Salmonella* (Verma et al., 2015) (**Suppl. Figure**  
461 **S11d**). At 7-hours post infection, we observed *Salmonella* in the perinuclear region of these  
462 cells. The expression of IL-8 was also seen to go up in these cells which is one of the  
463 hallmarks of *Salmonella* infection. Interestingly, a concordant increase in the expression of  
464 Kdm6B (**Suppl. Figure S11e**) was also observed.

465 Activation of Kdm6B is known to regulate a large set of genes and thereby modulate  
466 fundamental programs of a cell including proliferation and differentiation. To investigate  
467 such a role of Kdm6B role in bestowing tumor related properties in gallbladder cells, we  
468 tested cell proliferation and cell migratory properties. We experimentally perturbed Kdm6B  
469 expression in NOZ cells to examine this. Plasmids encoding Kdm6B or its catalytic mutant

470 (KDM6B<sup>H1390A</sup>) were transfected into NOZ cells followed by cell proliferation assay.  
471 Successful transfection of constructs in NOZ cells was confirmed by RT-PCR (**Figure 6B**).  
472 We observed that cells overexpressing wild-type Kdm6B showed a >2-fold increase in cell  
473 proliferation, while no change was observed in case of Catalytic mutant (CM) of Kdm6B  
474 (**Suppl. Figure S12**). Next, we carried out siRNA mediated knockdown of Kdm6B which  
475 also resulted in decreased cell proliferation compared to scrambled siRNA transfected control  
476 (**Suppl. Figure S12**). Next, treatment with demethylase inhibitor, GSKJ4, at 15uM and 30uM  
477 resulted in decreased cell proliferation in a concentration dependent manner (**Suppl. Figure**  
478 **S12**). In line with this, wound healing assay revealed a higher rate of wound closure in case  
479 of cells treated with wild-type Kdm6B compared to its CM at all the time points i.e. 12, 24  
480 and 32 hrs (**Suppl. Figure S12**) a phenotype that was also seen upon GSKJ4 treatment in  
481 comparison to the respective controls at 12, 24 and 32 hrs post treatment (**Suppl. Figure**  
482 **S12**).

483 Next, a sub-cutaneous tumour model with NOZ cells was used to examine the role of Kdm6B  
484 in gallbladder tumorigenesis. The NOZ cells were injected subcutaneously into NOD/SCID  
485 mice followed by intraperitoneal injection of GSKJ4 (**Suppl. Figure S13**). Post-xenografting,  
486 the growth of the xenograft in the control mice showed a steady increase. However, in  
487 contrast, GSKJ4 treatment resulted in regression of tumor growth as evidenced by animal  
488 body weight, tumour volume and weight (**Suppl. Figure S13**). Taken together these data  
489 strongly indicate initiation of pro-tumorigenic mechanism in a Kdm6B dependent manner  
490 during *Salmonella* infection.

491

## 492 **Discussion:**

493 Carcinogenesis is a multifactorial process involving primarily genetic susceptibility and  
494 environmental factors. However, genetic and environmental factors may not account for the  
495 entire cancer risk and therefore chronic microbial infection might be the 3<sup>rd</sup> important co-  
496 factor, referred to as a tripartite multidimensional interaction by the International Cancer  
497 Microbiome Consortium (Scott et al, 2019). Many chronic microbial infections such as the  
498 human papilloma virus, the hepatitis B virus, and *Helicobacter pylori* infection have been  
499 shown to be definite carcinogens (Masrouroudsari et al. 2017). In the case of gallbladder  
500 cancer, chronic *Salmonella* infection has also been suggested as a co-factor in its  
501 carcinogenesis (Iyer et al., 2016; Scanu et al., 2015; Shukla et al., 2000; Upadhyay et al.,  
502 2022). Chronic *Salmonella* carrier state has been associated with GBC in many historical  
503 studies, including more recent studies based on *Salmonella* Vi antibodies (Welton et al, 1979;

504 Mellemegaard et al, 1988; Dutta et al, 2000). A meta-analysis of >1000 patients with GBC  
505 showed a relative risk of 4.6 (95% CI: 3.1–6.8) for anti-Vi antibodies positive individuals  
506 (Koshiol et al, 2016). However, Vi antibody seropositivity may not reflect *Salmonella*  
507 infection in the gallbladder. Detection of *Salmonella* in the GBC tissue is difficult by the  
508 culture technique and therefore the association remains weak. Furthermore, whether the  
509 association of chronic *Salmonella* infection with GBC is causal or not has not been proven.  
510 Does *Salmonella* reside in the gallbladder in a state called ‘dynamic symbiosis’ with cancer  
511 occurring mainly due to random DNA replication errors (Tomasetti et al. 2017) or the chronic  
512 *Salmonella* infection contributes significantly to carcinogenesis and requires robust  
513 association and mechanistic studies.

514 In the present study, we looked at the association of chronic *Salmonella* infection with  
515 GBC in human studies and developed a murine model to get a mechanistic insight into the  
516 pathogenesis of how chronic infection might contribute to GBC.

517 In the case-control study, we found that *Salmonella enterica* was present in the fecal  
518 microbiome of patients with GBC whereas it was absent in healthy controls. This has not  
519 been reported previously. We then studied whether *Salmonella* was present in the GBC  
520 tissue. Using a 16S rRNA based targeted metagenomic approach, we found the presence of *S.*  
521 Typhimurium in the gallbladder cancer tissue. A few studies have earlier shown the presence  
522 of *Salmonella typhi* in the GBC tissue (Pratap et al 2013; Scanu et al 2015; Nath et al 2008).  
523 Notably, detection of the non-typhoidal *Salmonellae* was also reported (Iyer et al., 2016). The  
524 presence of microbial infection, both bacteria and fungus, within the cancer tissue has been  
525 linked with carcinogenesis e.g. *Malassezia* spp. in pancreatic cancer (Thomas et al. 2018;  
526 Aykut et al, 2019). *Salmonella* may reside for long in the gallbladder through a biofilm  
527 formation and thus contribute to GBC (Di Domenico et al, 2017).

528 *S. Typhimurium* being a non-typhoidal serovar, has been predominantly causing gastro-  
529 intestinal infections worldwide. Over the past decade, invasive non-typhoidal *Salmonella*  
530 (iNTS) associated blood stream infections have been reported widely in Africa, with two-  
531 thirds due to *S. Typhimurium* (Marchello et al., 2019). These were the multidrug resistant  
532 phenotypes that belonged to the sequence type of ST313, that differed from ST19 by 700  
533 SNPs (Kingsley et al., 2009; Okoro et al., 2012, Feasey et al., 2015). In India, ST19 was the  
534 most common iNTS serovar, while a single case of iNTS ST313 was also reported (Jacob et  
535 al., 2019, Jacob et al., 2020). To the best of our knowledge, here we report for the first time  
536 the invasive ST19 *S. Typhimurium* that was associated with gallbladder cancer in the Indian  
537 patients.



538 The genomes of *S. Typhimurium* isolated from the gallbladder tissue have been analyzed in  
539 detail for the host adaptation genomic signatures, as ST19 were predominantly associated  
540 with gastrointestinal diseases. We identified certain key signatures that could have led this  
541 pathogen to become invasive in crossing the intestinal mucosal surface. Among the top 10  
542 signatures that led ST313 to become more invasive, eight genes were conserved in all the 28  
543 GBC isolates (Pulford et al., 2021) whereas, two pseudogenes in ST313 *ratB* and *sseI* were  
544 also found to be inactivated in GBC isolates. Inactivation of *ratB* reduces the enteric potential  
545 and *sseI* increases the rapid dissemination ability of the bacteria to the lymph nodes from the  
546 gut (Okoro et al., 2015; Carden et al., 2017).

547 *S. Typhimurium* harbors effector proteins of SPI-1 and SPI-2 T3SS, which are known to  
548 induce proinflammatory signalling and trigger inflammation (Bruno et al., 2009). The  
549 virulence of *S. Typhimurium* was shown to be conferred by two inducible prophages (Gifsy1-  
550 2) (Figuroa-Bossi N et al., 1999). In the present study, the GBC tissue isolates contained  
551 mainly three functional prophage sequences (Gifsy1-2, STM64) and four phage remnants  
552 (Def1-4) having virulence genes encoded in them. *gogB* from Gifsy-1 phage has a protease  
553 activity by targeting the NF- $\kappa$ B transcription factors RELA and RELB, thereby reducing the  
554 inflammatory response to *S. Typhimurium*. It is believed that this anti-inflammatory property  
555 will reduce tissue damage during long-term infection, whereas inflammation that lasts for a  
556 short time may enhance colonization in the intestine (Pilar et al., 2012).

557 At least two virulence genes have been reported to be carried by Gifsy-2 phage. The first  
558 being *sodCl* and the second is an unidentified factor(s). *sodCl* is responsible for encoding one  
559 of the two periplasmic Cu/Zn superoxide dismutases of bacteria *Salmonella* (Farrant et al.,  
560 1997, De Groote et al., 1997). These phage and phage remnants are known to play an  
561 important role in infection (Stanley et al., 2000, Figuroa-Bossi N et al., 2001). Almost 88%  
562 of *S. Typhimurium* are reported to carry a 90Kb virulence plasmid (Helmuth et al., 1985). In  
563 our study, four virulence plasmids were identified in the GBC tissue isolates which carry  
564 known virulence genes. PlasmidP02 and plasmid3 carried *entD* (enterobactin) as the  
565 virulence gene whereas CFSAN002003 plasmid, also a virulence plasmid, is encoded by  
566 *pefC*, *spvB*, *spvC*, *pefD*, *rck*, *pefA*, *pefB* virulence factor genes. The molecular functions of  
567 *spvB*, *spvC* are not clearly known although *spvB* is known to be involved in secretion (Gulig  
568 et al., 1993). Another region on the plasmid included a plasmid encoded fimbriae loci known  
569 as *pef*, which is involved in adhesion of bacteria to epithelial cells of the intestine (Baumler et  
570 al., 1999) and lastly a *rck* gene responsible for resistance to complement killing (Heffernan et  
571 al., 1992).

572 With regard to the mechanistic insight, we found that gallstones induced chronic  
573 inflammation in the murine model, but when these mice were infected with *Salmonella*, they  
574 developed significantly greater chronic inflammation in the gallbladder. In the chronic model  
575 when the infection was prolonged, the GB epithelium developed pre-malignant changes.  
576 These findings are similar to our previous observations in human gallbladder stones disease,  
577 where gallstones-induced chronic inflammation also led to development of pre-neoplastic  
578 lesions (Jain et al., 2014).

579 The molecular mechanisms through which microbial infection may be involved in  
580 carcinogenesis are complex and not well understood except in a few instances e.g. HPV and  
581 HBV infection. Chronic inflammation, immune interactions, and genotoxicity may be the  
582 primary drivers of carcinogenesis.

583 Inflammation is at the core of carcinogenesis, underlying many microbial associations with  
584 cancer e.g. *H. pylori* and gastric cancer (Francescone R et al., 2014). Microbial virulence  
585 factors induce chronic inflammation in the host tissue, stimulating cellular proliferation.  
586 Pathogen-associated molecular patterns (PAMPs) induce proinflammatory effects by acting  
587 on host pattern recognition receptors, such as toll-like (TLR) and nucleotide-binding  
588 oligomerization domain-like (NOD) receptors. Downstream activation of cell survival  
589 pathways may contribute to carcinogenesis even remotely (Dapito DH et al, 2012).

590 In the murine gallbladder, significant inflammation was induced by the chronic *Salmonella*  
591 infection in the present study. Three important proinflammatory SPI-1-T3SS effector  
592 proteins sopE2, sopB/sigD and sopA were found in *S. Typhimurium* by others (Hapfelmeier  
593 S et al., 2004; Zhang Y et al., 2006; Thien K et al., 2007). Immune modulation also  
594 contributes to the persistence of infection and chronic inflammation. *S. Typhimurium*, which  
595 harbours *galU*, a glucosylphosphate uridyl transferase gene may cause immune modulation.

596 Many bacteria produce toxins, which might cause DNA, damage e.g. Cytolethal distending  
597 toxin (CDT) and colibactin produced by *Escherichia coli* and *Campylobacter jejuni* induce  
598 DNA breaks (N esić D et al., 2004). *S. Typhi* has been shown to produce such CDT. At the  
599 molecular level mostly three genes are responsible for the formation of cytolethal toxins i.e.,  
600 CdtA, CdtB, and CdtC. CdtB gene is responsible for carcinogenic activity and creates the  
601 double-stranded DNA break in host cell DNA (Upadhayay et al., 2022). But *S. Typhimurium*  
602 lacks the gene for these toxins. Instead, it produces another toxin AvrA which has been  
603 shown to be involved in functional modulation of host *p53*. The significance of this  
604 modification in the context of gallbladder cancer is not fully known and needs future  
605 investigation. Rck, another protein encoded by *Salmonella Typhimurium* was shown to cause

606 DNA double stranded breaks thereby imparting cyclomodulin with a genotoxic activity  
607 (Mambu J et al., 2020).

608 In an earlier study, we showed that chronic *Salmonella* infection could induce  
609 epigenetic changes in the murine model. The involvement of Kdm6B, a histone demethylase,  
610 is necessary for a successful chronic *Salmonella* infection. In the present study, we also  
611 demonstrate that histone demethylase KDM6B recruitment on the PPAR $\delta$  promoter results in  
612 the loss of the H3K27me3 mark leading to its transcriptional activation. PPAR $\delta$  is a fatty acid  
613 oxidation regulator that modulates macrophage polarization, favoring the M2 spectrum and  
614 resulting in *Salmonella* chronic infection (Rana et al., 2021). Our human transcriptomics data  
615 suggest that several genes such as *ADAMTSL5*, *CX3CR1*, *HMGA2*, *MMP7*, *EPHB2*, *TYMP*,  
616 *HLA-A*, *MK167*, *HDGF* are differentially regulated in the tumor tissue samples from  
617 gallbladder cancer patients as compared to the normal epithelium in patients with gallstones.  
618 Functional analysis through KEGG showed that differentially expressed genes were related to  
619 metabolic pathways, neutrophil extracellular trap formation, alcoholism and transcriptional  
620 mis-regulation in cancer. A recently published study from China also showed that the mRNA  
621 expression profile change significantly at various stages of gallbladder cancer, and lipid-  
622 based metabolic abnormalities play an important role (Yang S et al., 2023). To discern their  
623 role in the context of *Salmonella* infection, several potential cancer associated candidates,  
624 which were significantly dysregulated, were further analysed. The data showed the  
625 importance of these genes in gallbladder tumorigenesis. One of the identified proteins  
626 ADAMTSL5, is a modulator of extracellular matrix. Interestingly, in our study the promoter  
627 region of ADAMTSL5 was found to be epigenetically modulated by KDM6B. KDM6B  
628 mediated remodeling of ADAMTSL5 promoter region was seen. In a recent work,  
629 ADAMTSL5 was reported to be associated with signalling of hepatocellular carcinoma,  
630 suggesting it to act as a master regulator of tumorigenicity (Arechederra et al., 2021).  
631 Although we have shown that chronic *Salmonella* infection may contribute to GB  
632 carcinogenesis, there could be other bacteria or co-factors that might also play an important  
633 role, as suggested by the ‘alpha-bug hypothesis’ (Sears CL et al., 2011) or the ‘driver-  
634 passenger model’ (Tjalsma H et al., 2012) where a dominant microbe by itself may play a  
635 necessary but not sufficient role and could lead to other changes in the microenvironment that  
636 promote carcinogenesis. Although we could not fulfil Koch’s postulate, it is difficult to apply  
637 Koch’s postulate to cancers that are multifactorial in origin, and chronic infection could be  
638 one of the important factors.

639 Taken together, our findings suggest that there is a strong causal association between  
640 GBC and a particular type of chronic *Salmonella* Typhimurium infection (ST19), which  
641 probably originates from the gut, colonizes the gallbladder, induces chronic inflammation  
642 because of its virulence and causes epigenetic changes leading to gallbladder carcinogenesis.  
643 Our findings might explain the high incidence of GBC in northern India, where typhoid fever  
644 is endemic and the prevalence of gallbladder stones is ~5% in the general population.

645

## 646 **Methods**

647 The study was conducted after obtaining due clearance from the Institute Ethics Committee.  
648 Informed written consent was taken from all human participants.

### 649 **Human Participants:**

650 Group A: Patients with histology proven GBC were included as cases

651 Group B: Patients with gallbladder stone diseases were included as diseased controls

### 652 **Inclusion criteria of cases and controls:**

- 653 • Age 18-60 years
- 654 • No obstructive jaundice
- 655 • No prior surgical or endoscopic intervention

### 656 **Exclusion criteria:**

- 657 • Use of antibiotics in the preceding 4 weeks
- 658 • Use of Proton pump inhibitors in the preceding 4 weeks
- 659 • Metastatic disease
- 660 • Serum bilirubin >2 mg/dL
- 661 • Major comorbid illness, uncontrolled diabetes

662 **Diagnosis of GBC:** The diagnosis of GBC was suspected clinically and on imaging (contrast  
663 enhanced computed tomography scan of the abdomen), and confirmed on cytology or  
664 histopathology. The diagnosis of gallstone disease was made on an ultrasound examination of  
665 the abdomen.

666 **Fecal and gallbladder tissue samples collection for microbiome study:** Fecal sample was  
667 collected from the cases and controls after explaining the method of sample collection in a sterile  
668 container-containing sample transport buffer BiomLife (Ruhvenile Biomedical, India). Each  
669 participant was provided with a sterile plastic sheet and a sterile container with spoon. They were  
670 asked to get their hands and genital area cleaned with soap and water. In a dry place, the sterile

671 plastic sheet was opened just before defecation. Patient was advised to defecate at the center of  
672 the sheet without touching it. Then a scoop of fecal sample was taken with the spoon (approx.  
673 3g) and transferred to the container-containing sample transport buffer BiomLife. The container  
674 was tightly closed and immediately transferred to 4°C before transporting to the laboratory and  
675 frozen at -80°C within 4 hrs. Like fecal samples, gallbladder tissues were also collected in sterile  
676 BiomLife transport buffer for metagenomic DNA extraction and microbiome study.

#### 677 **16S rRNA based fecal microbiome diversity and statistical analysis:**

678 Gut and gallbladder tissue microbiome of study subjects was investigated by 16S rRNA  
679 based targeted metagenomic sequencing. The quality of NGS reads covering V3-V4 regions  
680 of 16S rRNA gene were evaluated and merged by fastp program by keeping Phred Quality  
681 Score(Q)  $\geq 20$ , read length  $\geq 50$ , and removing 10 bases from head and tail. The fastp program  
682 has also merging facility of paired reads. So, all quality passed paired reads were merged and  
683 used to generate operational taxonomic units (OTUs) by QIIME2-2021.11 pipeline (Bolyen  
684 et al., 2019). Two R version 3.6.1 packages, ggplot2 and ampViz2 were used to perform  
685 statistical analysis.

#### 686 **Quality assessment of NGS data**

687 The quality of paired read generated from MiSeq platform was examined by FastQC version  
688 0.11.9 program (Andrews, S. 2010). All paired reads were filtered by setup Phred Quality  
689 Score (Q)  $\geq 20$ , read length  $\geq 36$ , and removing 10 bases from the most sequencing error prone  
690 region i.e., head and tail of each read. These parameters were implemented in Trimmomatic  
691 program ver0.39 (Bolger et al, 2014) to get high quality reads.

#### 692 **Isolation, confirmation and cultivation of *Salmonella Typhimurium* from Gall bladder** 693 **Tissue samples**

694 Tissue samples from GBC patients were obtained during surgical resection of the tumor,  
695 which were confirmed by histology. The tumor tissue was collected in BHI medium and  
696 immediately transported to the lab at room temp. Collected tissues were enriched in 3 ml of  
697 BHI medium in aerobic conditions at 37° C. Following 6 hours incubation, 4 to 5 sterile glass  
698 beads (3.00 mm) were added into the medium and vortex gently for detaching cells from the  
699 tissue. Approximately, 300  $\mu$ l culture aliquot was utilized for plating on the Heketon enteric  
700 agar plates. All the plates were incubated at 37°C for 48 hours. At least three colonies from  
701 each plate were confirmed by complete 16S rRNA gene sequencing from ten different GBC  
702 patients.

## 703 **Whole genome sequencing, quality assessment, assembling and annotation**

704 Whole genome sequencing (WGS) was performed by a high-throughput next-generation  
705 Illumina MiSeq sequencing platform (*in-house*) and Nextera XT DNA Library preparation kit  
706 (Illumina, Inc., USA). High-quality raw reads (Q>30) were used for *de-novo* assembly by  
707 SPAdes v3.15.3 (Bankevich et al, 2012). The assembled genomes were annotated using  
708 Rapid Annotation using Subsystem Technology (RAST) version 2.0. The genomes were  
709 submitted in NCBI database. A global representation of *S. Typhimurium* deposited in  
710 Enterobase database has been included for comparative genomics with all the genomes  
711 downloaded from <https://enterobase.warwick.ac.uk/species/index/senterica>. At the time of  
712 this analysis, a total of 39565 *S. Typhimurium* genomes were available (as on 09.03.2022).  
713 For the present study, only genomes that had information for source, year and place of  
714 isolation sourced from humans have been considered. This yielded a total of 3665 genomes  
715 that fulfilled all the inclusion criteria, with STs belonging to eburst group 1 (eBG) ST19,  
716 ST34 and ST313. MLST STs of the present study isolates were determined using the  
717 pubMLST database schemes with seven housekeeping genes (*aroC*, *dnaN*, *hemD*, *hisD*,  
718 *purE*, *sucA* and *thrA*) (<https://github.com/tseemann/mlst>).

## 719 **Phylogenetic analysis**

720 The genome assemblies of *S. Typhimurium* were mapped against the reference *S.*  
721 *Typhimurium* LT2 (Accession No. NC\_003197.2) using Snippy v4.6.0 (Seemann, 2015)  
722 (<https://github.com/tseemann/snippy>) (Seeman, 2015). The core genome SNP differences  
723 against the reference and as well within the genomes were generated as a core alignment file.  
724 SNPs were extracted from the core alignment <https://github.com/sanger-pathogens/snp-sites>,  
725 which was then subjected to construct a maximum likelihood (ML) phylogenetic analysis  
726 through RaxML with GTRGAMMA model (Stamatakis et al., 2014). The generated phylogeny  
727 was then rooted against the reference genome *S. Typhimurium* LT2, visualized and annotated  
728 with the metadata using iTOL (Letunic and Bork, 2019). Among the 3665 genomes included  
729 in the preliminary analysis, genomes that were identical and sourced from an outbreak  
730 clusters were removed. The final genomes that were included in the further analysis were  
731 2517, with 28 and 2489 genomes from GBC and global representatives respectively.

## 732 **Mutational profiling**

733 The presence of any type of nucleotide variation as mutations in the form of single nucleotide  
734 polymorphisms (SNPs), insertions or deletions was identified *in-silico* using snippy pipeline  
735 with mapping and variant calling features. To obtain the mutational profile, the genomes

736 assemblies were compared against annotated reference genome *S. Typhimurium* LT2  
737 (Accession No. NC\_003197.2). Mutation accumulation was manually curated with the  
738 respective STs included in the study. Importantly, genes that were inactivated by means of  
739 either missense mutations or an insertion/deletion leading to frameshift mutations were  
740 analyzed. Any such mutations that resulted in the loss of functionality of the protein were  
741 termed as hypothetically disrupted coding sequences (HDCS) or pseudogenes. These genes  
742 were compared with the HDCS host adaptation signatures of the invasive ST313 lineages.

#### 743 **Pan genome analysis**

744 The pan genome analysis was performed for all the 2517 genomes and reference LT2. The  
745 genomes were annotated using Prokka v. 1.14 (Seemann et al., 2014), with the genus  
746 database “*Salmonella*” (<https://github.com/tseemann/prokka>). The GFF files that were  
747 generated from prokka was taken to assess the genome diversity of the 2517 genomes using  
748 panaroo (Tonkin-Hill et al., 2020) (<https://github.com/gtonkinhill/panaroo>) (Tonkin-Hill et  
749 al., 2020). Panaroo was run with “strict” mode option that enables to retain genes that were  
750 present at least in 5% of all the genomes being analysed. The gene presence/absence results  
751 obtained from panaroo was run through twilight scripts and grouped as GBC invasive ST19  
752 (n=28), global sources: ST19 (n=1880), ST34 (n=418) and ST313 (n=191)  
753 (<https://github.com/ghoresh11/twilight>) (Horesh et al., 2021)

#### 754 ***In-silico* identification of plasmid and prophage sequences**

755 PLSDB was used to check for the plasmid and plasmid replicons within the studied genome  
756 of *S. Typhimurium*, n=28 (Galata et al., 2019). The analysis was completed using Mash  
757 (search strategy: mash screen) with a maximal p-value of 0.1 and minimal identity of 0.99.  
758 To remove redundancy from the output data, the winner-takes-all strategy was applied. 28  
759 genomes from *S. Typhimurium* were analyzed for the presence of prophage sequences using  
760 PHASTER (PHAge Search Tool Enhanced Release) (<http://phaster.ca/>) web server (Arndt et  
761 al., 2016). It is a upgradation of the PHAST webserver for the fast identification of prophage  
762 sequences present within the bacterial genome (Zhou et al., 2011). Both the plasmid and  
763 prophage sequences were further confirmed for its presence in the studied *S. Typhimurium*  
764 genomes through BLASTn manually.

#### 765 **Detection of virulence factors in the genome of *S. Typhimurium***

766 Virulence factor database (VFDB) was used for the detection of putative virulence factors in  
767 the *S. Typhimurium* genome (n=28) isolated from GBC tissue samples (Liu et al., 2022). VF  
768 analyser tool available at VFDB are developed in Java-Script rich manner. The work flow  
769 proceeds by construction of orthologous groups within the query genome and the previously

770 analysed *S. Typhimurium* strain LT2 as the representative genome to get rid of false positive  
771 results. Next it carries out repetitive similarity searches for the accurate detection of virulence  
772 factors (VF). Eventually a data refinement process is carried out for VF encoded by gene  
773 clusters (Liu et al., 2022). We also manually carried out BLASTn searches for the  
774 proinflammatory and anti-inflammatory virulence genes present in the reference *S.*  
775 *Typhimurium* LT2 genome with our draft genome assemblies and compared it with the  
776 results of VF analyser. The virulence genes encoding virulence factors for the reference strain  
777 LT2 were downloaded from VFDF dataset. Heatmap representing virulence genes were  
778 prepared in R software.

### 779 **Genome-wide expression profiling of human GBC:**

780 Tissue samples were collected from GBC and gallstone patients during surgery. Each sample  
781 was divided and put into two tubes: one containing RNA later and the other containing formalin.  
782 Samples in RNA later were initially stored at 4° C for 24 hours and then stored at -80° C.  
783 Tissue samples in formalin were processed for block formation. H&E staining was done to  
784 confirm the presence of tumor area.

785 Total-RNA extraction from tissue was standardized using organic method (Ambion extraction  
786 kit).

787 **Controls:** We included histologically normal mucosa from patients with gallbladder stones as  
788 control.

### 789 **RNA extraction and quality check**

790 RNA extraction was done using mirVana microRNA isolation kit (Ambion). The quality of  
791 extracted RNA was checked by nanodrop and 260/280 value ranged between 1.8 to 2.0.  
792 Quality and integrity of extracted RNA was also checked using Agilent 2100 Bioanalyzer,  
793 RNA 6000 Nano LabChip kit and Agilent 2100 Expert Software (Agilent Technologies,  
794 Santa Clara, CA, USA). Samples with RNA integrity number (RIN) more than or equal to 6.5  
795 were selected for further analysis.

### 796 **Microarray experiment**

797 The protocol of one-color micro-array-based gene expression (Agilent technologies;  
798 SurePrint G3 Human Gene Expression 8x60K v2 Microarray) was followed as per  
799 manufacturer's recommendations. Hybridized arrays were scanned with Agilent's G2505B  
800 microarray scanner system and the raw data was collected. Out of 35 samples collected, the  
801 microarray dataset consisted of 32 samples, of which 16 samples were control and 16 were  
802 from adenocarcinoma patients.

### 803 **Differential gene expression analysis**



804 The microarray data generated from Agilent platform belonged to two categories  
805 adenocarcinoma (adeno) and the control group. The LIMMA (Bioconductor;  
806 <https://www.bioconductor.org/>) package has been used to convert the probe level data into  
807 the expression measures and DEGs were analyzed in the adeno vs control group. DEGs were  
808 reported using the criteria of fold-change  $\geq 1.5$  and fold change  $< -1.5$  by conducting t-test  
809 with adjusted p value of  $< 0.05$ , characterized as upregulated and downregulated genes.  
810 Benjamini Hochberg correction was applied.

811 For functional analysis, KEGG (Kyoto Encyclopaedia of Genes and Genomes)  
812 (<http://www.kegg.jp/>) analysis was performed on differentially expressed genes to understand  
813 the pathways involved.  
814

### 815 **Experimental murine studies:**

816 **A. Preparation of *S. Typhimurium* bacterial culture for infection:** Fresh *S. Typhimurium*  
817 (SL1344 and SL3261 are laboratory strain) was revived from  $-80^{\circ}\text{C}$  storage and streaked on  
818 a fresh Luria Bertani (LB) Agar plate. On the day before experiment, a single colony was  
819 picked from the LB agar plate and inoculated to a 2 ml of Luria broth (LB) taken in a sterile  
820 falcon tube and grown at  $37^{\circ}\text{C}$  with aeration. For secondary culture, grown primary culture  
821 was added to 12 ml of LB at 1:1000 dilution and was grown over night at  $37^{\circ}\text{C}$  without  
822 shaking. On the day of infection, cells were pelleted at 4000 rpm for 10 min and washed with  
823 filtered 1X PBS for two times and resuspended in 1 ml 1X PBS. The bacteria were then  
824 added to tissue culture plate containing mammalian cells at MOI of 1:40 for NOZ cells and  
825 MOI of 1:10 for primary gallbladder cells isolated from mice gallbladder.  
826

827 **B. Cell and culture conditions:** Human gallbladder carcinoma cell line NOZ (procured  
828 from JCRB Cell Bank - Japanese Collection of Research Bioresources Cell Bank) were  
829 grown in DMEM media (Sigma) supplemented with 14 mM  $\text{NaHCO}_3$  (Sigma), 15 mM  
830 HEPES buffer (pH 7.4) (GIBCO), 1 mM sodium pyruvate (GIBCO), 40 mg/ L penicillin  
831 (GIBCO), 90 mg/L streptomycin (GIBCO), and 10% fetal bovine serum (GIBCO).  
832 Gallbladder primary cell line were prepared from C57BL/6 as previously described (Rahul  
833 Kuver; 1996). All cell cultures were incubated in humidified  $37^{\circ}\text{C}$  incubator with 5%  $\text{CO}_2$ .  
834

835 **C. *Salmonella Typhimurium* infection of cultured mammalian cells:** Cells were grown  
836 and seeded in tissue culture treated appropriate well plates. Upon attaining confluency, cells  
837 were washed and again supplemented with antibiotic free media. NOZ Cells were then  
838 infected with *S. Typhimurium* SL1344 as mentioned above at MOI 1:40 and gallbladder  
839 primary cells at MOI of 1:10. This setup was incubated at  $37^{\circ}\text{C}$  for 1 h. Following incubation,  
840 bacteria were washed off two times with media and resuspended again in fresh media  
841 containing 100ug/ml gentamicin for 1 h at  $37^{\circ}\text{C}$ . After 1hr, media was again removed and

842 fresh media with 10ug/ml gentamicin was supplemented. Cells were then incubated for the  
843 rest of period of infection at 37<sup>0</sup> C in CO<sub>2</sub>incubator. The cells were then harvested for protein  
844 and RNA which were further analysed by western blot and real time PCR.

845

846 **D. *Salmonella in vivo* chronic carriage gallstone model:** The FVB/N mice of 3-4 weeks  
847 were taken and grouped into Control, SL infected, Lithogenic diet (LD) and Lithogenic diet  
848 plus *Salmonella* infected (LD-SL). LD and LD-SL grouped mice were fed for 9 weeks a  
849 lithogenic diet i.e. 1% cholesterol and 0.5% cholic acid mixed with the normal diet. Post 9  
850 weeks, the chronic infection causing bacteria SL3261ΔaroA was fed orally to mice at 10<sup>9</sup>  
851 CFU by gavage. Mice were euthanized at different time intervals (15 days, 4 months, 8.5  
852 months, 1.5 years and 1.8 years) post infection and gallbladder was taken out and processed  
853 for histopathological study, RNA, and protein. For subcutaneous tumor mice model, GSKJ4  
854 drug treatment was given at a dose of 1mg/Kg of mice body weight intraperitoneally (ip) on  
855 alternative days for 1 month. Appropriate drug control and untreated control were included in  
856 the study.

857

858 **E. Immunoblotting:** Protein samples were prepared from respective mice tissue and  
859 mentioned cell lines by lysis with RIPA lysis buffer (Sigma R0278) and 1X protease inhibitor  
860 cocktail (G-Biosciences). The cell lysates prepared were quantified using CBX protein assay  
861 kit (G-Bioscience, USA). Equal amount of protein was resolved on sodium dodecyl sulfate-  
862 polyacrylamide gel electrophoresis (SDS-PAGE) and then transferred to nitrocellulose  
863 membrane. Blots were probed with appropriate antibodies.

864

865 **F. RNA extraction and quantitative real-time PCR (qRT-PCR):** Total RNA were isolated  
866 from mice tissues, human GBC cell line NOZ and organoids using Nucleo Spin RNA-II Kit  
867 (MN, Germany) according to the manufacturer's protocol. One microgram of total RNA from  
868 each sample was used to synthesize cDNA using i-Script cDNA synthesis Kit (Bio-Rad,  
869 USA). Bio-Rad CFX 96TM Real-Time Detection System was used for real-time PCR (qRT-  
870 PCR) using i-Taq Syber green (BioRad, USA) according to manufacturer's instruction. Gene  
871 expression levels were normalized according to the average cycle threshold values for the  
872 internal control gene HPRT. Cycle threshold values were extracted and data analysis was  
873 performed using the ΔΔCt method.

874

875 **G. Histopathology and Immunohistochemistry:** In order to perform histopathology and  
876 immunohistochemistry of gallbladder tissue, sections of tissue were fixed in 10% formalin  
877 overnight and embedded in parafilm. Sections of 5 mm thickness were cut onto glass slides  
878 and processed using Cryotome (Thermo) and were stained with hematoxylin and eosin  
879 (H&E) and evaluated under a light microscope with attached DP25 digital camera. For IHC,

880 the tissue glass slides were washed using 1X PBS for three times (5 minutes each). Further,  
881 the endogenous peroxidase activity was quenched by treating the tissue with 3% H<sub>2</sub>O<sub>2</sub> for 20  
882 minutes. The tissue sample or cells were again washed using 1X PBS for two times (5  
883 minutes each), then blocked with 5% goat serum at room temperature for one hour. The  
884 sections were incubated with primary antibodies prepared in 5% goat serum overnight in a  
885 moist chamber. Sections were washed with 1X PBS for three times at 5 minutes each and  
886 were incubated with secondary HRP conjugate antibody for 2 hours prepared in 5% goat  
887 serum at room temperature in a moist chamber. The tissues were washed three times using  
888 1X PBS. For immunohistochemistry, the slides were stained with DAB substrate (Sigma,  
889 USA) and counterstained with Haematoxylin. Images were taken on a Nikon Fluorescence  
890 Microscope using colour camera.

891

892 **H. Cell migration using wound healing assay:** The KDM6B gene knockdown and knocked  
893 down effect on cell migration was examined using wound healing assay. NOZ cells were  
894 plated at a density of  $1.5 \times 10^5$ /well in DMEM with 1% FBS in a 24-well plate and cultured.  
895 After approximately 24 hours of incubation, the cells were transfected with KDM6B WT and  
896 catalytic deficient plasmid. Next, the monolayer were scraped in a straight line to create a  
897 'scratch' with a p200 pipette tip as reported earlier (Mustafa *et. al.*, 2017). Plates were then  
898 incubated and monitored periodically by microscopy to examine wound and migration of  
899 cells in transfected and un-transfected cells.

900

901 **I. Cell proliferation assay:** NOZ cells were seeded ( $1.5 \times 10^5$  cells /well) onto the cell  
902 culture plates. After approximately 24 hours of incubation, the cells were transfected with  
903 KDM6B WT and catalytic deficient plasmid. Next, these cells were split on the 6 well plates  
904 after counting equal no. of cells i.e. 1000 per well. After 1 week, the bottom surface of the  
905 plate was stained with 0.1% crystal violet and quantified using a light microscope.

906

907 **J. ChIP qPCR expression analysis:**

908 NOZ cells were grown to confluency of 80-90% and infected with *Salmonella* for 18 hrs as  
909 described previously. Post 18 hrs of infection, the cells were cross linked with 1%  
910 formaldehyde at RT for 10 mins. Crosslinking was stopped by addition of 125mM glycine to  
911 quench formaldehyde. The cells were collected and washed with PBS 3 times. Cells were  
912 then lysed with lysis buffer (PBS + 0.1% NP40 + protease inhibitor) to obtain nucleus. The  
913 nuclei were lysed using nucleus lysis buffer for 10 mins on ice. The lysed samples were  
914 sheared using a sonicator to obtain chromatin fragments of 200-500 bp. Sheared chromatin  
915 was subjected to immunoprecipitation using ChIP grade antibodies specific for KDM6B,  
916 Histone3 K27me3 and IgG control acting as negative control overnight at 4°C. The  
917 immunoprecipitated DNA was pulled using Protein G sepharose beads through incubation at

918 4°C for 3 hrs. The immunoprecipitated DNA and the input DNA were purified. qRT-PCR  
919 was performed using shortlisted promoter sequences of wnt pathway genes.

920

#### 921 **K. PCR identification for *Salmonella* isolates**

922 To detect the persistence of *Salmonella* in the mice, different organs were isolated and  
923 bacterial burden assay was performed in the above- described mouse model system. Mice  
924 were euthanized post infection and gallbladder and liver were harvested and homogenized in  
925 PBS (.1% triton X-100). The homogenized tissues were then serially diluted and plated onto  
926 Brilliant green agar and Hekton agar plates. The plates were incubated in a 37-degree  
927 incubator and bacterial CFU counted. All animal experiments were carried out in the Animal  
928 Facility of Regional Center for Biotechnology (RCB). Animal ethics proposal were approved  
929 by the RCB Institutional Animal Ethics Committee (approval no. IAEC/RCB/2021/102 and  
930 IAEC/RCB/ 2019/062).

#### 931 **L. Statistical Analysis:**

932 All results are expressed as the mean standard error from an individual experiment done in  
933 triplicate. Data were analyzed with one way ANOVA followed by standard unpaired two-  
934 tailed Student's t-test, Tukey's post-test and the Mann-Whitney U-test as applicable, with p-  
935 values of <0.05–0.001 were considered statistically significant. We used GraphPad PRISM  
936 for statistical analysis.

937

938 **Acknowledgement:** This research is supported by Intramural research grants by All India  
939 Institute of Medical Sciences, New Delhi to Pramod Kumar Garg, Kajal Jain, Asuri Krishna  
940 and VK Bansal. Dr. Pramod Kumar Garg is supported by the JC Bose fellowship by the  
941 Science & Engineering Research Board. Ethics clearances from the following IBSC, IAEC  
942 and IEC were obtained: (IEC-495/02.08.2019, RCB/IAEC/2019/062, RCB/IAEC/2021/102,  
943 RCB/IBSC/21-22/341, RCB-BBB-IEC-HI-31, RCB/IBSC/22-23/405, RCB/IAEC/2023/158,  
944 RCB/IBSC/23-24/480). We also thank the instrumentation facility at RCB and Small animal  
945 facility at NCR-Biotech Science Cluster. BD acknowledges Department of Biotechnology,  
946 Govt. of India for financial support (No. BT/PR30159/MED/15/188/2018). Authors  
947 acknowledge Mr. Subhash Tanwar, Mr. Roshan Kumar and Advanced Nucleotide  
948 Sequencing Facility of THSTI for microbial genome sequencing.

949

950 **Author contributions:** PKG conceived the idea; PKG, CVS, BD, KJ designed the  
951 experiments, supervised research, arranged resources and wrote the paper; AKP, SM, KJ, SP,

952 CR, SK, AP, DP, KK, DT, ANS, JV, PJ, SR, PK, AK, RY, BD performed experiments and  
953 contributed in the preparation of manuscript draft. SK, VKB provided clinical resources,  
954 designed experiments and helped in data analysis. All the authors approved the final  
955 manuscript.

956

957 **Declaration of interests:** Authors declared that there are no financial or other competing  
958 interests.

959

960 **Figure legends:**

961 **Figure 1:** Boxplot is displaying relative abundance of 10 bacterial phyla. The y- and x-axis  
962 represent relative abundance and phylum name, respectively. The statistical significance  
963 value was calculated by ANOVA for each phylum among three groups. The significant value  
964 (p-value) viz. 'ns' denotes non-significant. '\*', '\*\*', '\*\*\*' and '\*\*\*\*' represent the level of  
965 significant as  $\leq 0.05$ ,  $\leq 0.001$ ,  $\leq 0.0001$ , and  $\leq 0.00001$ , respectively.

966 **Figure 2: (a)** Maximum likelihood phylogenetic analysis of *S. Typhimurium* isolated from  
967 gallbladder tissues of GBC patients and compared with the global collection of 2490  
968 genomes. Scale bar indicates number of substitution per genome/per site. **(b)** sub-tree  
969 showing the high level resolution of the sub-cluster of ST19 genomes of GBC with other  
970 genomes from the global collection

971 **Figure 3: (a)** Dot plot shows the invasive index score of each of the *S. Typhimurium* isolates  
972 that was determined against the non-invasive reference *S. Typhimurium* genome LT2. **(b)**  
973 shows the distribution chart for the mutation frequency categorized as frameshift, missense,  
974 synonymous and others.

975 **Figure 4:** Pan genome analysis plots of 2518 *S. Typhimurium* genomes. **(a)** Phandango  
976 visualization of phylogenetic tree with the presence/absence gene profile, **(b)** sub-  
977 classification of the gene categories with respect to the distribution frequency, **(c)** mean  
978 distribution frequency as classified with different STs, **(d)** number of gene distributed with  
979 different STs groups.

980 **Figure 5. Development of murine model of gallstone and chronic *Salmonella* infection**  
981 [A] Schematic representation of the steps involved in development of Gallstone mice along  
982 with chronic *Salmonella* infection model Post *Salmonella* (ST) infection at the indicated time,  
983 the mice were euthanized followed by isolation of gallbladder, spleen and liver. Labels: C for  
984 mock-infected and normal diet fed control group, ST for *Salmonella* infection group, LD for  
985 Lithogenic diet (involving 1% cholesterol and 0.5% Cholic acid) group, LD-ST for

986 Lithogenic diet and Salmonella infection group. [B] Gallbladders from the indicated group  
987 along with magnified view of the generated gallstones (inset) are represented. [C]  
988 Splenomegaly seen in infected mice along with enlarged liver seen with change in color in  
989 Gallstones. [D] Agarose gel electrophoresis image post PCR amplification of DNA from  
990 isolated bacterial colonies cultured from infected mice (15 days post infection) from liver  
991 tissue using *Salmonella* Typhimurium 16S specific primers. [E] Agarose gel images of  
992 similar experiment carried out as previous figure with Fecal pellets to record shedding of  
993 *Salmonella*. DNA of *Salmonella* Typhimurium strain SL1344 was used as a positive control  
994 (+) and non DNA template was used as a negative control (-).

995 **Figure 6. Detection of Histopathological alterations in Gallstone mice model.**

996 Representative images of Hematoxylin and Eosin stained gallbladder sections from the  
997 indicated groups. The infection with *Salmonella* was for either 4 months [A.] or 8.5 months  
998 [B.] The epithelial lining of gallbladder is marked by blue arrowheads, inflammation by  
999 arrowheads, fibrosis by black arrowheads, metaplasia by green arrowheads, and hyperplasia  
1000 by arrowheads. The values of each of these parameters were quantified as histopathological  
1001 score by a pathologist blinded to the group and plotted (Right panel). [C.] Periodic acid  
1002 Schiff (PAS) staining of representative sections of the gallbladder of all the groups 4 months  
1003 post *Salmonella* infection indicating presence of higher amounts of acidic mucins in LD-ST  
1004 mice.

1005 **Figure 7. Alteration of epigenetic modulator KDM6B involved in maintenance of**  
1006 **H3K27me3 mark upon *Salmonella* Typhimurium infection.** Representation of KDM6B

1007 mRNA upregulation 15 days post ST infection, HPRT used for normalization of the data [A.]  
1008 Immunoblot representing KDM6B upregulation in gallbladder tissue of different indicated  
1009 groups of mice post infection of indicated duration. Expression analysis of P16 [C.] and  
1010 P53[D.] [B.] Immunoblot representing increased Kdm6B expression in gallbladder cancer  
1011 patient tissue (labelled with GBC1-3) compared to those from non-malignant control samples  
1012 (labelled as NMC1-3) and gallstone control samples (labelled as GS1-3). Expression analysis  
1013 of various genes [F.] Chromatin immunoprecipitation assay carried out using Kdm6B [G.],  
1014 H3K27me3 [H.] and [I.] histone H3 antibodies for binding in ADAMTSL5 gene promoter  
1015 post 18 hrs of *Salmonella* Typhimurium (SL1344) infection. Data representing fold  
1016 enrichment was plotted in each case. Expression analysis of ADAMTSL5 in murine  
1017 gallbladder post 15 days of *Salmonella* Typhimurium (SL1344 strain) infection represented  
1018 in fold change values by Real Time PCR. HPRT was used for normalization [J.].

1019 **Figure 8: (a)** Photograph showing cut-open gallbladder (GB) with liver margin (L) having  
1020 multiple growth/tumor (Tu) arising from fundus and two calculi (Ca). The region around the  
1021 calculi appears to be free of tumor (PN). **(b)** Representative hematoxylin & eosin staining of  
1022 a representative sample of gallbladder cancer **(c)** Post-extraction, total-RNA samples run on  
1023 1.5% agarose gel and bio-analyzer electropherogram of representative RNA sample **(d)**  
1024 Volcano plot showing differentially expressed transcripts (480; 327 up-regulated and 153  
1025 down-regulated) in GBC patient samples compared to gallstone controls. **(e)** Functional  
1026 analysis through KEGG pathway: KEGG enrichment analysis of differentially expressed  
1027 genes (DEGs) between GBC and gallbladder with stones. X-axis represent the number of  
1028 genes. The p-values for all the genes were significant but the corrected p-value was not found  
1029 to be significant.

1030  
1031  
1032  
1033  
1034

1035 **References**

- 1036 1. Arechederra, M., Bazai, S. K., Abdouni, A., Sequera, C., Mead, T. J., Richelme, S.,  
 1037 Daian, F., Audebert, S., Dono, R., Lozano, A., Gregoire, D., Hibner, U., Allende, D.  
 1038 S., Apte, S. S., & Maina, F. (2021). ADAMTSL5 is an epigenetically activated gene  
 1039 underlying tumorigenesis and drug resistance in hepatocellular carcinoma. *Journal of*  
 1040 *Hepatology*, 74(4), 893–906. <https://doi.org/10.1016/j.jhep.2020.11.008>
- 1041 2. Arndt, D., Grant, J. R., Marcu, A., Sajed, T., Pon, A., Liang, Y., & Wishart, D. S.  
 1042 (2016). PHASTER: A better, faster version of the PHAST phage search tool. *Nucleic*  
 1043 *Acids Research*, 44(W1), W16–W21. <https://doi.org/10.1093/nar/gkw387>
- 1044 3. Attili, A. F., De Santis, A., Capri, R., Repice, A. M., Maselli, S., & Group, G. (1995).  
 1045 The natural history of gallstones: The GREPCO experience. *Hepatology*, 21(3), 656–  
 1046 660. <https://doi.org/10.1002/hep.1840210309>
- 1047 4. Aykut, B., Pushalkar, S., Chen, R., Li, Q., Abengozar, R., Kim, J. I., Shadaloey, S. A.,  
 1048 Wu, D., Preiss, P., Verma, N., Guo, Y., Saxena, A., Vardhan, M., Diskin, B., Wang,  
 1049 W., Leinwand, J., Kurz, E., Kochen Rossi, J. A., Hundeyin, M., ... Miller, G. (2019).  
 1050 The fungal mycobiome promotes pancreatic oncogenesis via activation of MBL.  
 1051 *Nature*, 574(7777), 264–267. <https://doi.org/10.1038/s41586-019-1608-2>
- 1052 5. Bankevich, A., Nurk, S., Antipov, D., Gurevich, A. A., Dvorkin, M., Kulikov, A. S.,  
 1053 Lesin, V. M., Nikolenko, S. I., Pham, S., Prjibelski, A. D., Pyshkin, A. V., Sirotkin,  
 1054 A. V., Vyahhi, N., Tesler, G., Alekseyev, M. A., & Pevzner, P. A. (2012). SPAdes: A  
 1055 New Genome Assembly Algorithm and Its Applications to Single-Cell Sequencing.  
 1056 *Journal of Computational Biology*, 19(5), 455–477.  
 1057 <https://doi.org/10.1089/cmb.2012.0021>
- 1058 6. Batra, Y., Pal, S., Dutta, U., Desai, P., Garg, P. K., Makharia, G., Ahuja, V., Pande,  
 1059 G. K., Sahni, P., Chattopadhyay, T. K., & Tandon, R. K. (2005). Gallbladder cancer  
 1060 in India: A dismal picture. *Journal of Gastroenterology and Hepatology*, 20(2), 309–  
 1061 314. <https://doi.org/10.1111/j.1440-1746.2005.03576.x>
- 1062 7. Bolger, A. M., Lohse, M., & Usadel, B. (2014). Trimmomatic: A flexible trimmer for  
 1063 Illumina sequence data. *Bioinformatics*, 30(15), 2114–2120.  
 1064 <https://doi.org/10.1093/bioinformatics/btu170>
- 1065 8. Bolyen, E., Rideout, J. R., Dillon, M. R., Bokulich, N. A., Abnet, C. C., Al-Ghalith,  
 1066 G. A., Alexander, H., Alm, E. J., Arumugam, M., Asnicar, F., Bai, Y., Bisanz, J. E.,  
 1067 Bittinger, K., Brejnrod, A., Brislawn, C. J., Brown, C. T., Callahan, B. J., Caraballo-  
 1068 Rodríguez, A. M., Chase, J., ... Caporaso, J. G. (2019). Reproducible, interactive,  
 1069 scalable and extensible microbiome data science using QIIME 2. *Nature*  
 1070 *Biotechnology*, 37(8), 852–857. <https://doi.org/10.1038/s41587-019-0209-9>
- 1071 9. Bruno, V. M., Hannemann, S., Lara-Tejero, M., Flavell, R. A., Kleinstein, S. H., &  
 1072 Galán, J. E. (2009). Salmonella Typhimurium Type III Secretion Effectors Stimulate  
 1073 Innate Immune Responses in Cultured Epithelial Cells. *PLoS Pathogens*, 5(8),  
 1074 e1000538. <https://doi.org/10.1371/journal.ppat.1000538>
- 1075 10. Carden, S. E., Walker, G. T., Honeycutt, J., Lugo, K., Pham, T., Jacobson, A.,  
 1076 Bouley, D., Idoyaga, J., Tsohis, R. M., & Monack, D. (2017). Pseudogenization of the



- 1077 Secreted Effector Gene *sslI* Confers Rapid Systemic Dissemination of *S.*  
 1078 Typhimurium ST313 within Migratory Dendritic Cells. *Cell Host & Microbe*, 21(2),  
 1079 182–194. <https://doi.org/10.1016/j.chom.2017.01.009>
- 1080 11. Chang, M.-H. (2014). Prevention of hepatitis B virus infection and liver cancer.  
 1081 *Recent Results in Cancer Research. Fortschritte Der Krebsforschung. Progres Dans*  
 1082 *Les Recherches Sur Le Cancer*, 193, 75–95. [https://doi.org/10.1007/978-3-642-38965-](https://doi.org/10.1007/978-3-642-38965-8_5)  
 1083 [8\\_5](https://doi.org/10.1007/978-3-642-38965-8_5)
- 1084 12. Chen, M., Zou, S., He, C., Zhou, J., Li, S., Shen, M., Cheng, R., Wang, D., Zou, T.,  
 1085 Yan, X., Huang, Y., & Shen, J. (2020). Transactivation of SOX5 by Brachyury  
 1086 promotes breast cancer bone metastasis. *Carcinogenesis*, 41(5), 551–560.  
 1087 <https://doi.org/10.1093/carcin/bgz142>
- 1088 13. Crawford, R. W., Rosales-Reyes, R., Ramírez-Aguilar, M. D. L. L., Chapa-Azuela,  
 1089 O., Alpuche-Aranda, C., & Gunn, J. S. (2010). Gallstones play a significant role in  
 1090 *Salmonella* spp. Gallbladder colonization and carriage. *Proceedings of the National*  
 1091 *Academy of Sciences*, 107(9), 4353–4358. <https://doi.org/10.1073/pnas.1000862107>
- 1092 14. Dapito DH, Mencin A, Gwak GY, et al. Promotion of hepatocellular carcinoma by the  
 1093 intestinal microbiota and TLR4. *Cancer Cell* 2012; 21:504–16.  
 1094
- 1095 15. De Groote, M. A., Ochsner, U. A., Shiloh, M. U., Nathan, C., McCord, J. M.,  
 1096 Dinauer, M. C., Libby, S. J., Vazquez-Torres, A., Xu, Y., & Fang, F. C. (1997).  
 1097 Periplasmic superoxide dismutase protects *Salmonella* from products of phagocyte  
 1098 NADPH-oxidase and nitric oxide synthase. *Proceedings of the National Academy of*  
 1099 *Sciences*, 94(25), 13997–14001. <https://doi.org/10.1073/pnas.94.25.13997>
- 1100 16. Di Domenico, E. G., Cavallo, I., Pontone, M., Toma, L., & Ensoli, F. (2017). Biofilm  
 1101 Producing *Salmonella* Typhi: Chronic Colonization and Development of Gallbladder  
 1102 Cancer. *International Journal of Molecular Sciences*, 18(9), 1887.  
 1103 <https://doi.org/10.3390/ijms18091887>
- 1104 17. Ding, S.-Z., Goldberg, J. B., & Hatakeyama, M. (2010). *Helicobacter pylori* infection,  
 1105 oncogenic pathways and epigenetic mechanisms in gastric carcinogenesis. *Future*  
 1106 *Oncology*, 6(5), 851–862. <https://doi.org/10.2217/fon.10.37>
- 1107 18. Dutta, U., Garg, P. K., Kumar, R., & Tandon, R. K. (2000). Typhoid carriers among  
 1108 patients with gallstones are at increased risk for carcinoma of the gallbladder. *The*  
 1109 *American Journal of Gastroenterology*, 95(3), 784–787.  
 1110 <https://doi.org/10.1111/j.1572-0241.2000.01860.x>
- 1111 19. Dutta, U., Nagi, B., Garg, P. K., Sinha, S. K., Singh, K., & Tandon, R. K. (2005).  
 1112 Patients with gallstones develop gallbladder cancer at an earlier age: *European*  
 1113 *Journal of Cancer Prevention*, 14(4), 381–385. [https://doi.org/10.1097/00008469-](https://doi.org/10.1097/00008469-200508000-00011)  
 1114 [200508000-00011](https://doi.org/10.1097/00008469-200508000-00011)
- 1115 20. Ethun, C. G., Le, N., Lopez-Aguilar, A. G., Pawlik, T. M., Poultsides, G., Tran, T.,  
 1116 Idrees, K., Isom, C. A., Fields, R. C., Krasnick, B. A., Weber, S. M., Salem, A.,  
 1117 Martin, R. C. G., Scoggins, C. R., Shen, P., Mogal, H. D., Schmidt, C., Beal, E.,  
 1118 Hatzaras, I., ... Maithel, S. K. (2017). Pathologic and Prognostic Implications of

- 1119 Incidental versus Nonincidental Gallbladder Cancer: A 10-Institution Study from the  
1120 United States Extrahepatic Biliary Malignancy Consortium. *The American Surgeon*,  
1121 83(7), 679–686. <https://www.ncbi.nlm.nih.gov/pmc/articles/PMC5915617/>
- 1122 21. Everhart, J. E., & Ruhl, C. E. (2009). Burden of Digestive Diseases in the United  
1123 States Part III: Liver, Biliary Tract, and Pancreas. *Gastroenterology*, 136(4), 1134–  
1124 1144. <https://doi.org/10.1053/j.gastro.2009.02.038>
- 1125 22. Farrant, J. L., Sansone, A., Canvin, J. R., Pallen, M. J., Langford, P. R., Wallis, T. S.,  
1126 Dougan, G., & Kroll, J. S. (1997). Bacterial copper- and zinc-cofactored superoxide  
1127 dismutase contributes to the pathogenesis of systemic salmonellosis. *Molecular*  
1128 *Microbiology*, 25(4), 785–796. <https://doi.org/10.1046/j.1365-2958.1997.5151877.x>
- 1129 23. Feasey, N. A., Masesa, C., Jassi, C., Faragher, E. B., Mallewa, J., Mallewa, M.,  
1130 MacLennan, C. A., Msefula, C., Heyderman, R. S., & Gordon, M. A. (2015). Three  
1131 Epidemics of Invasive Multidrug-Resistant *Salmonella* Bloodstream Infection in  
1132 Blantyre, Malawi, 1998–2014. *Clinical Infectious Diseases*, 61(suppl 4), S363–S371.  
1133 <https://doi.org/10.1093/cid/civ691>
- 1134 24. Figueroa-Bossi, N., & Bossi, L. (1999). Inducible prophages contribute to *Salmonella*  
1135 virulence in mice. *Molecular Microbiology*, 33(1), 167–176.  
1136 <https://doi.org/10.1046/j.1365-2958.1999.01461.x>
- 1137 25. Figueroa-Bossi, N., Uzzau, S., Maloriol, D., & Bossi, L. (2001). Variable assortment  
1138 of prophages provides a transferable repertoire of pathogenic determinants in  
1139 *Salmonella*. *Molecular Microbiology*, 39(2), 260–272. <https://doi.org/10.1046/j.1365-2958.2001.02234.x>
- 1141 26. Francescone R, Hou V, Microbiome GSI. inflammation, and cancer. *Cancer J* 2014;  
1142 20:181–9.
- 1143 27. Galata, V., Fehlmann, T., Backes, C., & Keller, A. (2019). PLSDB: A resource of  
1144 complete bacterial plasmids. *Nucleic Acids Research*, 47(D1), D195–D202.  
1145 <https://doi.org/10.1093/nar/gky1050>
- 1146 28. Gulig, P. A., Danbara, H., Guiney, D. G., Lax, A. J., Norel, F., & Rhen, M. (1993).  
1147 Molecular analysis of spv virulence genes of the salmonella virulence plasmids.  
1148 *Molecular Microbiology*, 7(6), 825–830. <https://doi.org/10.1111/j.1365-2958.1993.tb01172.x>
- 1150 29. Heberle, H., Meirelles, G. V., Da Silva, F. R., Telles, G. P., & Minghim, R. (2015).  
1151 InteractiVenn: A web-based tool for the analysis of sets through Venn diagrams. *BMC*  
1152 *Bioinformatics*, 16(1), 169. <https://doi.org/10.1186/s12859-015-0611-3>
- 1153 30. Heffernan, E. J., Reed, S., Hackett, J., Fierer, J., Roudier, C., & Guiney, D. (1992).  
1154 Mechanism of resistance to complement-mediated killing of bacteria encoded by the  
1155 *Salmonella typhimurium* virulence plasmid gene rck. *Journal of Clinical*  
1156 *Investigation*, 90(3), 953–964. <https://doi.org/10.1172/JCI115972>
- 1157 31. Helmuth, R., Stephan, R., Bunge, C., Hoog, B., Steinbeck, A., & Bulling, E. (1985).  
1158 Epidemiology of virulence-associated plasmids and outer membrane protein patterns

- 1159 within seven common Salmonella serotypes. *Infection and Immunity*, 48(1), 175–182.  
1160 <https://doi.org/10.1128/iai.48.1.175-182.1985>
- 1161 32. Hiley, L., Graham, R. M. A., & Jennison, A. V. (2019). Genetic characterisation of  
1162 variants of the virulence plasmid, pSLT, in Salmonella enterica serovar Typhimurium  
1163 provides evidence of a variety of evolutionary directions consistent with vertical  
1164 rather than horizontal transmission. *PLOS ONE*, 14(4), e0215207.  
1165 <https://doi.org/10.1371/journal.pone.0215207>
- 1166 33. Horesh, G., Taylor-Brown, A., McGimpsey, S., Lassalle, F., Corander, J., Heinz, E.,  
1167 & Thomson, N. R. (2021). Different evolutionary trends form the twilight zone of the  
1168 bacterial pan-genome. *Microbial Genomics*, 7(9).  
1169 <https://doi.org/10.1099/mgen.0.000670>
- 1170 34. Hulsege, I., Kommadath, A., & Smits, M. A. (2009). Globaltest and GOEAST: Two  
1171 different approaches for Gene Ontology analysis. *BMC Proceedings*, 3(S4), S10.  
1172 <https://doi.org/10.1186/1753-6561-3-S4-S10>
- 1173 35. Iyer, P., Barreto, S. G., Sahoo, B., Chandrani, P., Ramadwar, M. R., Shrikhande, S.  
1174 V., & Dutt, A. (2016). Non-typhoidal Salmonella DNA traces in gallbladder cancer.  
1175 *Infectious Agents and Cancer*, 11(1), 12. <https://doi.org/10.1186/s13027-016-0057-x>
- 1176 36. Jacob, J. J., Anandan, S., Venkatesan, M., Neeravi, A., Vasudevan, K., Pragasam, A.  
1177 K., & Veeraraghavan, B. (2019). Genomic analysis of human invasive Salmonella  
1178 enterica serovar Typhimurium ST313 isolate B3589 from India. *Infection, Genetics  
1179 and Evolution*, 73, 416–424. <https://doi.org/10.1016/j.meegid.2019.05.023>
- 1180 37. Jacob, J. J., Solaimalai, D., Muthuirulandi Sethuvel, D. P., Rachel, T., Jeslin, P.,  
1181 Anandan, S., & Veeraraghavan, B. (2020). A nineteen-year report of serotype and  
1182 antimicrobial susceptibility of enteric non-typhoidal Salmonella from humans in  
1183 Southern India: Changing facades of taxonomy and resistance trend. *Gut Pathogens*,  
1184 12(1), 49. <https://doi.org/10.1186/s13099-020-00388-z>
- 1185 38. Jain, K., Mohapatra, T., Das, P., Misra, M. C., Gupta, S. D., Ghosh, M., Kabra, M.,  
1186 Bansal, V. K., Kumar, S., Sreenivas, V., & Garg, P. K. (2014). Sequential Occurrence  
1187 of Preneoplastic Lesions and Accumulation of Loss of Heterozygosity in Patients  
1188 With Gallbladder Stones Suggest Causal Association With Gallbladder Cancer.  
1189 *Annals of Surgery*, 260(6), 1073–1080.  
1190 <https://doi.org/10.1097/SLA.0000000000000495>
- 1191 39. Jain, K., Sreenivas, V., Velpandian, T., Kapil, U., & Garg, P. K. (2013). Risk factors  
1192 for gallbladder cancer: A case-control study. *International Journal of Cancer*, 132(7),  
1193 1660–1666. <https://doi.org/10.1002/ijc.27777>
- 1194 40. Kingsley, R. A., Msefula, C. L., Thomson, N. R., Kariuki, S., Holt, K. E., Gordon, M.  
1195 A., Harris, D., Clarke, L., Whitehead, S., Sangal, V., Marsh, K., Achtman, M.,  
1196 Molyneux, M. E., Cormican, M., Parkhill, J., MacLennan, C. A., Heyderman, R. S., &  
1197 Dougan, G. (2009). Epidemic multiple drug resistant *Salmonella* Typhimurium  
1198 causing invasive disease in sub-Saharan Africa have a distinct genotype. *Genome  
1199 Research*, 19(12), 2279–2287. <https://doi.org/10.1101/gr.091017.109>

- 1200 41. Koshiol, J., Wozniak, A., Cook, P., Adaniel, C., Acevedo, J., Azócar, L., Hsing, A.  
 1201 W., Roa, J. C., Pasetti, M. F., Miquel, J. F., Levine, M. M., Ferreccio, C., the  
 1202 Gallbladder Cancer Chile Working Group, Aguayo, C. G., Baez, S., Díaz, A., Molina,  
 1203 H., Miranda, C., Castillo, C., ... Hildesheim, A. (2016). *Salmonella enterica* serovar  
 1204 Typhi and gallbladder cancer: A case-control study and meta-analysis. *Cancer*  
 1205 *Medicine*, 5(11), 3310–3235. <https://doi.org/10.1002/cam4.915>
- 1206 42. Letunic, I., & Bork, P. (2019). Interactive Tree Of Life (iTOL) v4: Recent updates  
 1207 and new developments. *Nucleic Acids Research*, 47(W1), W256–W259.  
 1208 <https://doi.org/10.1093/nar/gkz239>
- 1209 43. Liu, B., Zheng, D., Zhou, S., Chen, L., & Yang, J. (2022). VFDB 2022: A general  
 1210 classification scheme for bacterial virulence factors. *Nucleic Acids Research*, 50(D1),  
 1211 D912–D917. <https://doi.org/10.1093/nar/gkab1107>
- 1212 44. Lou, L., Zhang, P., Piao, R., & Wang, Y. (2019). Salmonella Pathogenicity Island 1  
 1213 (SPI-1) and Its Complex Regulatory Network. *Frontiers in Cellular and Infection*  
 1214 *Microbiology*, 9, 270. <https://doi.org/10.3389/fcimb.2019.00270>
- 1215 45. Mambu, J., Barilleau, E., Fragnet-Trapp, L., Le Vern, Y., Olivier, M., Sadrin, G.,  
 1216 Grépinet, O., Taieb, F., Velge, P., & Wiedemann, A. (2020). Rck of Salmonella  
 1217 Typhimurium Delays the Host Cell Cycle to Facilitate Bacterial Invasion. *Frontiers in*  
 1218 *Cellular and Infection Microbiology*, 10, 586934.  
 1219 <https://doi.org/10.3389/fcimb.2020.586934>
- 1220 46. Marchello, C. S., Dale, A. P., Pisharody, S., Rubach, M. P., & Crump, J. A. (2019). A  
 1221 Systematic Review and Meta-analysis of the Prevalence of Community-Onset  
 1222 Bloodstream Infections among Hospitalized Patients in Africa and Asia.  
 1223 *Antimicrobial Agents and Chemotherapy*, 64(1), e01974-19.  
 1224 <https://doi.org/10.1128/AAC.01974-19>
- 1225 47. Maringhini, A. (1987). Gallstones, Gallbladder Cancer, and Other Gastrointestinal  
 1226 Malignancies: An Epidemiologic Study in Rochester, Minnesota. *Annals of Internal*  
 1227 *Medicine*, 107(1), 30. <https://doi.org/10.7326/0003-4819-107-1-30>
- 1228 48. Dudgaard, A., & Gaarslev, K. (1988). Risk of Hepatobiliary Cancer in Carriers of  
 1229 Salmonella typhi. *JNCI Journal of the National Cancer Institute*, 80(4), 288–288.  
 1230 <https://doi.org/10.1093/jnci/80.4.288>
- 1231 49. Nath, G., Singh, Y. K., Kumar, K., Gulati, A. K., Shukla, V. K., Khanna, A. K.,  
 1232 Tripathi, S. K., Jain, A. K., Kumar, M., & Singh, T. B. (2008). Association of  
 1233 carcinoma of the gallbladder with typhoid carriage in a typhoid endemic area using  
 1234 nested PCR. *The Journal of Infection in Developing Countries*, 2(04), 302–307.  
 1235 <https://doi.org/10.3855/jidc.226>
- 1236 50. N esić D, Hsu Y, Stebbins CE. Assembly and function of a bacterial genotoxin.  
 1237 *Nature* 2004; 429:429–33.
- 1238 51. Okoro, C. K., Barquist, L., Connor, T. R., Harris, S. R., Clare, S., Stevens, M. P.,  
 1239 Arends, M. J., Hale, C., Kane, L., Pickard, D. J., Hill, J., Harcourt, K., Parkhill, J.,  
 1240 Dougan, G., & Kingsley, R. A. (2015). Signatures of Adaptation in Human Invasive

- 1241 Salmonella Typhimurium ST313 Populations from Sub-Saharan Africa. *PLOS*  
 1242 *Neglected Tropical Diseases*, 9(3), e0003611.  
 1243 <https://doi.org/10.1371/journal.pntd.0003611>
- 1244 52. Okoro, C. K., Kingsley, R. A., Connor, T. R., Harris, S. R., Parry, C. M., Al-  
 1245 Mashhadani, M. N., Kariuki, S., Msefula, C. L., Gordon, M. A., de Pinna, E., Wain,  
 1246 J., Heyderman, R. S., Obaro, S., Alonso, P. L., Mandomando, I., MacLennan, C. A.,  
 1247 Tapia, M. D., Levine, M. M., Tennant, S. M., ... Dougan, G. (2012). Intracontinental  
 1248 spread of human invasive Salmonella Typhimurium pathovariants in sub-Saharan  
 1249 Africa. *Nature Genetics*, 44(11), 1215–1221. <https://doi.org/10.1038/ng.2423>
- 1250 53. Pilar, A. V. C., Reid-Yu, S. A., Cooper, C. A., Mulder, D. T., & Coombes, B. K.  
 1251 (2012). GogB Is an Anti-Inflammatory Effector that Limits Tissue Damage during  
 1252 Salmonella Infection through Interaction with Human FBXO22 and Skp1. *PLoS*  
 1253 *Pathogens*, 8(6), e1002773. <https://doi.org/10.1371/journal.ppat.1002773>
- 1254 54. Pratap, C. B., Kumar, G., Patel, S. K., Verma, A. K., Shukla, V. K., Kumar, K., &  
 1255 Nath, G. (2013). Targeting of putative fimbrial gene for detection of S. Typhi in  
 1256 typhoid fever and chronic typhoid carriers by nested PCR. *The Journal of Infection in*  
 1257 *Developing Countries*, 7(07), 520–527. <https://doi.org/10.3855/jidc.2561>
- 1258 55. Pulford, C. V., Perez-Sepulveda, B. M., Canals, R., Bevington, J. A., Bengtsson, R. J.,  
 1259 Wenner, N., Rodwell, E. V., Kumwenda, B., Zhu, X., Bennett, R. J., Stenhouse, G. E.,  
 1260 Malaka De Silva, P., Webster, H. J., Bengoechea, J. A., Dumigan, A., Tran-Dien, A.,  
 1261 Prakash, R., Banda, H. C., Alufandika, L., ... Hinton, J. C. D. (2021). Stepwise  
 1262 evolution of Salmonella Typhimurium ST313 causing bloodstream infection in  
 1263 Africa. *Nature Microbiology*, 6(3), 327–338. [https://doi.org/10.1038/s41564-020-](https://doi.org/10.1038/s41564-020-00836-1)  
 1264 [00836-1](https://doi.org/10.1038/s41564-020-00836-1)
- 1265 56. Raffatellu, M., Wilson, R. P., Chessa, D., Andrews-Polymenis, H., Tran, Q. T.,  
 1266 Lawhon, S., Khare, S., Adams, L. G., & Bäumlner, A. J. (2005). SipA, SopA, SopB,  
 1267 SopD, and SopE2 Contribute to *Salmonella enterica* Serotype Typhimurium Invasion  
 1268 of Epithelial Cells. *Infection and Immunity*, 73(1), 146–154.  
 1269 <https://doi.org/10.1128/IAI.73.1.146-154.2005>
- 1270 57. Rana, S., Maurya, S., Mohapatra, G., Singh, S., Babar, R., Chandrasekhar, H.,  
 1271 Chamoli, G., Rathore, D., Kshetrapal, P., & Srikanth, C. V. (2021). Activation of  
 1272 epigenetic regulator KDM6B by *Salmonella* Typhimurium enables chronic infections.  
 1273 *Gut Microbes*, 13(1), 1986665. <https://doi.org/10.1080/19490976.2021.1986665>
- 1274 58. Rolhion, N., Furniss, R. C. D., Grabe, G., Ryan, A., Liu, M., Matthews, S. A., &  
 1275 Holden, D. W. (2016). Inhibition of Nuclear Transport of NF-κB p65 by the  
 1276 Salmonella Type III Secretion System Effector SpvD. *PLOS Pathogens*, 12(5),  
 1277 e1005653. <https://doi.org/10.1371/journal.ppat.1005653>
- 1278 59. Rowland, R. H., Ian R. (2000). Metabolic Activities of the Gut Microflora in Relation  
 1279 to Cancer. *Microbial Ecology in Health and Disease*, 12(2), 179–185.  
 1280 <https://doi.org/10.1080/089106000750060431>
- 1281 60. Scanu, T., Spaapen, R. M., Bakker, J. M., Pratap, C. B., Wu, L., Hofland, I., Broeks,  
 1282 A., Shukla, V. K., Kumar, M., Janssen, H., Song, J.-Y., Neefjes-Borst, E. A., te Riele,

- 1283 H., Holden, D. W., Nath, G., & Neefjes, J. (2015). Salmonella Manipulation of Host  
 1284 Signaling Pathways Provokes Cellular Transformation Associated with Gallbladder  
 1285 Carcinoma. *Cell Host & Microbe*, 17(6), 763–774.  
 1286 <https://doi.org/10.1016/j.chom.2015.05.002>
- 1287 61. Sears CL, Pardoll DM. Perspective: alpha-bugs, their microbial partners, and the link  
 1288 to colon cancer. *J Infect Dis* 2011; 203:306–11.
- 1289 62. Seemann, T. (2014). Prokka: Rapid prokaryotic genome annotation. *Bioinformatics*,  
 1290 30(14), 2068–2069. <https://doi.org/10.1093/bioinformatics/btu153>
- 1291 63. Shaffer, E., & Hundal, R. (2014). Gallbladder cancer: Epidemiology and outcome.  
 1292 *Clinical Epidemiology*, 99. <https://doi.org/10.2147/CLEP.S37357>
- 1293 64. Sharma, A., Dwary, A. D., Mohanti, B. K., Deo, S. V., Pal, S., Sreenivas, V., Raina,  
 1294 V., Shukla, N. K., Thulkar, S., Garg, P., & Chaudhary, S. P. (2010). Best Supportive  
 1295 Care Compared With Chemotherapy for Unresectable Gall Bladder Cancer: A  
 1296 Randomized Controlled Study. *Journal of Clinical Oncology*.  
 1297 <https://doi.org/10.1200/JCO.2010.29.3605>
- 1298 65. Sharma, A., Sharma, K. L., Gupta, A., Yadav, A., & Kumar, A. (2017). Gallbladder  
 1299 cancer epidemiology, pathogenesis and molecular genetics: Recent update. *World*  
 1300 *Journal of Gastroenterology*, 23(22), 3978. <https://doi.org/10.3748/wjg.v23.i22.3978>
- 1301 66. Shukla, V. K., Singh, H., Pandey, M., Upadhyay, S. K., & Nath, G. (2000).  
 1302 Carcinoma of the gallbladder—Is it a sequel of typhoid? *Digestive Diseases and*  
 1303 *Sciences*, 45(5), 900–903. <https://doi.org/10.1023/a:1005564822630>
- 1304 67. Smyth, G. K. (2005). limma: Linear Models for Microarray Data. In R. Gentleman, V.  
 1305 J. Carey, W. Huber, R. A. Irizarry, & S. Dudoit (Eds.), *Bioinformatics and*  
 1306 *Computational Biology Solutions Using R and Bioconductor* (pp. 397–420). Springer-  
 1307 Verlag. [https://doi.org/10.1007/0-387-29362-0\\_23](https://doi.org/10.1007/0-387-29362-0_23)
- 1308 68. Song, C., Lv, J., Liu, Y., Chen, J. G., Ge, Z., Zhu, J., Dai, J., Du, L.-B., Yu, C., Guo,  
 1309 Y., Bian, Z., Yang, L., Chen, Y., Chen, Z., Liu, J., Jiang, J., Zhu, L., Zhai, X., Jiang,  
 1310 Y., ... for the China Kadoorie Biobank Collaborative Group. (2019). Associations  
 1311 Between Hepatitis B Virus Infection and Risk of All Cancer Types. *JAMA Network*  
 1312 *Open*, 2(6), e195718. <https://doi.org/10.1001/jamanetworkopen.2019.5718>
- 1313 69. Stamatakis, A. (2014). RAxML version 8: A tool for phylogenetic analysis and post-  
 1314 analysis of large phylogenies. *Bioinformatics*, 30(9), 1312–1313.  
 1315 <https://doi.org/10.1093/bioinformatics/btu033>
- 1316 70. Stanley, T. L., Ellermeier, C. D., & Slauch, J. M. (2000). Tissue-Specific Gene  
 1317 Expression Identifies a Gene in the Lysogenic Phage Gifsy-1 That Affects *Salmonella*  
 1318 *enterica* Serovar Typhimurium Survival in Peyer's Patches. *Journal of Bacteriology*,  
 1319 182(16), 4406–4413. <https://doi.org/10.1128/JB.182.16.4406-4413.2000>
- 1320 71. Stinton, L. M., & Shaffer, E. A. (2012). Epidemiology of Gallbladder Disease:  
 1321 Cholelithiasis and Cancer. *Gut and Liver*, 6(2), 172–187.  
 1322 <https://doi.org/10.5009/gnl.2012.6.2.172>

- 1323 72. Thomas, R. M., Gharaibeh, R. Z., Gauthier, J., Beveridge, M., Pope, J. L., Guijarro,  
1324 M. V., Yu, Q., He, Z., Ohland, C., Newsome, R., Trevino, J., Hughes, S. J., Reinhard,  
1325 M., Winglee, K., Fodor, A. A., Zajac-Kaye, M., & Jobin, C. (2018). Intestinal  
1326 microbiota enhances pancreatic carcinogenesis in preclinical models. *Carcinogenesis*,  
1327 39(8), 1068–1078. <https://doi.org/10.1093/carcin/bgy073>
- 1328 73. Tjalsma H, Boleij A, Marchesi JR, et al. A bacterial driver-passenger model for  
1329 colorectal cancer: beyond the usual suspects. *Nat Rev Microbiol* 2012; 10:575–82.
- 1330 74. Tomasetti, C., Li, L., & Vogelstein, B. (2017). Stem cell divisions, somatic mutations,  
1331 cancer etiology, and cancer prevention. *Science*, 355(6331), 1330–1334.  
1332 <https://doi.org/10.1126/science.aaf9011>
- 1333 75. Tonkin-Hill, G., MacAlasdair, N., Ruis, C., Weimann, A., Horesh, G., Lees, J. A.,  
1334 Gladstone, R. A., Lo, S., Beaudoin, C., Floto, R. A., Frost, S. D. W., Corander, J.,  
1335 Bentley, S. D., & Parkhill, J. (2020). Producing polished prokaryotic pangenomes  
1336 with the Panaroo pipeline. *Genome Biology*, 21(1), 180.  
1337 <https://doi.org/10.1186/s13059-020-02090-4>
- 1338 76. Unisa, S., Jagannath, P., Dhir, V., Khandelwal, C., Sarangi, L., & Roy, T. K. (2011).  
1339 Population-based study to estimate prevalence and determine risk factors of  
1340 gallbladder diseases in the rural Gangetic basin of North India. *HPB*, 13(2), 117–125.  
1341 <https://doi.org/10.1111/j.1477-2574.2010.00255.x>
- 1342 77. Upadhayay, A., Pal, D., & Kumar, A. (2022). Salmonella typhi induced oncogenesis  
1343 in gallbladder cancer: Co-relation and progression. *Advances in Cancer Biology -*  
1344 *Metastasis*, 4, 100032. <https://doi.org/10.1016/j.adcanc.2022.100032>
- 1345 78. Verma, S., Mohapatra, G., Ahmad, S. M., Rana, S., Jain, S., Khalsa, J. K., & Srikanth,  
1346 C. V. (2015). Salmonella Engages Host MicroRNAs To Modulate SUMOylation: A  
1347 New Arsenal for Intracellular Survival. *Molecular and Cellular Biology*, 35(17),  
1348 2932–2946. <https://doi.org/10.1128/MCB.00397-15>
- 1349 79. Welton, JohnC., Marr, JohnS., & Friedman, StephenM. (1979). ASSOCIATION  
1350 BETWEEN HEPATOBILIARY CANCER AND TYPHOID CARRIER STATE. *The*  
1351 *Lancet*, 313(8120), 791–794. [https://doi.org/10.1016/S0140-6736\(79\)91315-1](https://doi.org/10.1016/S0140-6736(79)91315-1)
- 1352 80. Zhou, Y., Liang, Y., Lynch, K. H., Dennis, J. J., & Wishart, D. S. (2011). PHAST: A  
1353 Fast Phage Search Tool. *Nucleic Acids Research*, 39(suppl), W347–W352.  
1354 <https://doi.org/10.1093/nar/gkr485>
- 1355 81. Zur Hausen, H. (2002). Papillomaviruses and cancer: From basic studies to clinical  
1356 application. *Nature Reviews Cancer*, 2(5), 342–350. <https://doi.org/10.1038/nrc798>
- 1357
- 1358 82. Howlader N, Noone AM, Krapcho M, et al., editors. SEER Cancer Statistics  
1359 Review. Bethesda, MD: National Cancer Institute; 1975-2014. Available  
1360 from:[https://seer.cancer.gov/csr/1975\\_2014/](https://seer.cancer.gov/csr/1975_2014/).

1361 83. National Cancer registry programme. Consolidated report of population based cancer  
1362 registries: 2012-14 [Internet]. Available online:  
1363 [http://ncdirindia.org/NCRP/ALL\\_NCRP\\_REPORTS/PBCR\\_REPORT\\_2012\\_2014/in](http://ncdirindia.org/NCRP/ALL_NCRP_REPORTS/PBCR_REPORT_2012_2014/index.htm)  
1364 [dex.htm](http://ncdirindia.org/NCRP/ALL_NCRP_REPORTS/PBCR_REPORT_2012_2014/index.htm)

1365 84. Yang S, Qin L, Wu P, Liu Y, Zhang Y, Mao B, Yan Y, Yan S, Tan F, Yue X, Liu H,  
1366 Xue H. (2023) RNA sequencing revealed the multi-stage transcriptome  
1367 transformations during the development of gallbladder cancer associated with chronic  
1368 inflammation. PLoS ONE, 18(3):e0283770  
1369

1370

1371

1372

1373

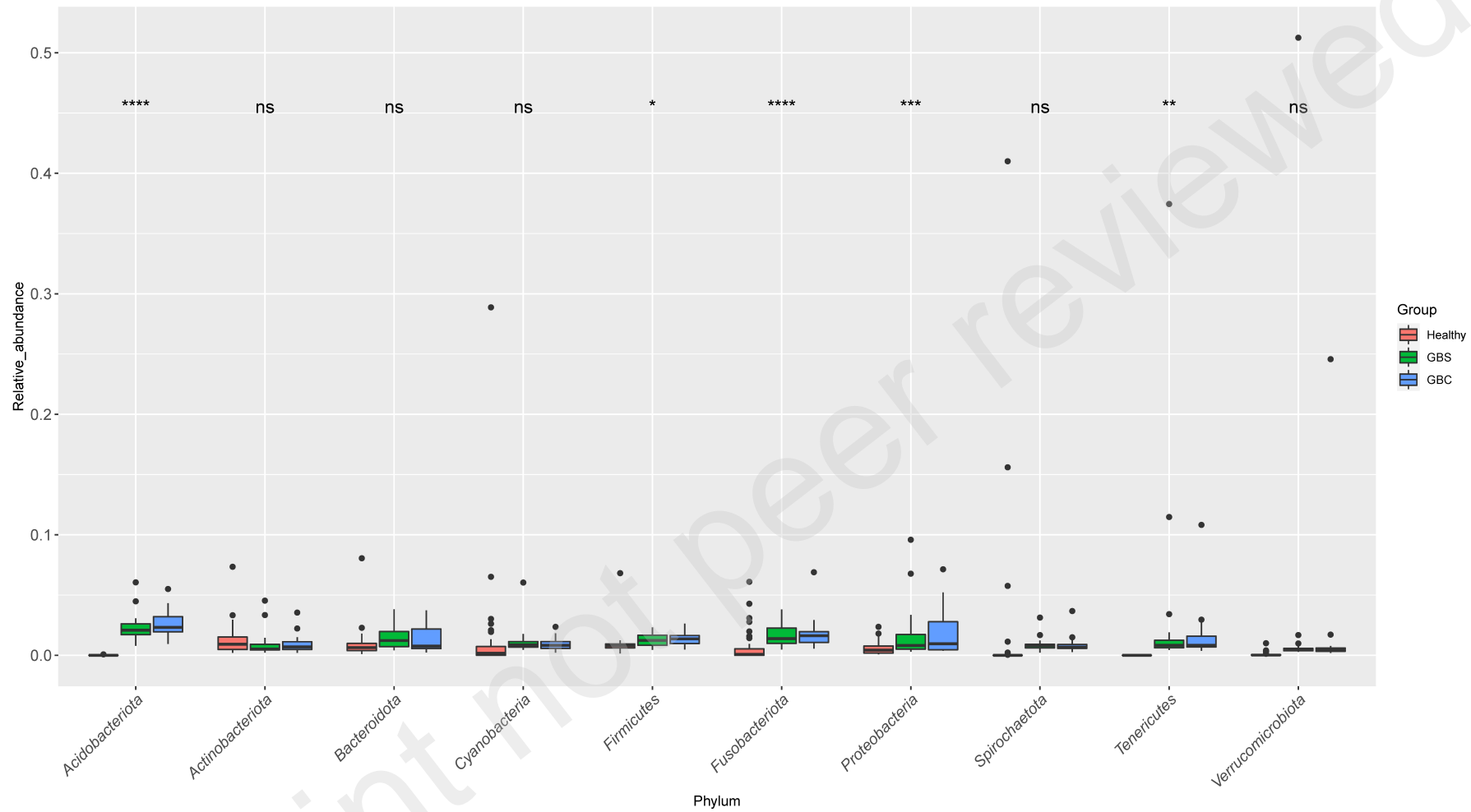
1374

1375

1376

1377





(a)

Tree scale: 0.01

1 Source\_of\_Isolation

- Faeces
- Blood
- Tissue
- Gall Bladder

2 Year\_of\_Isolation

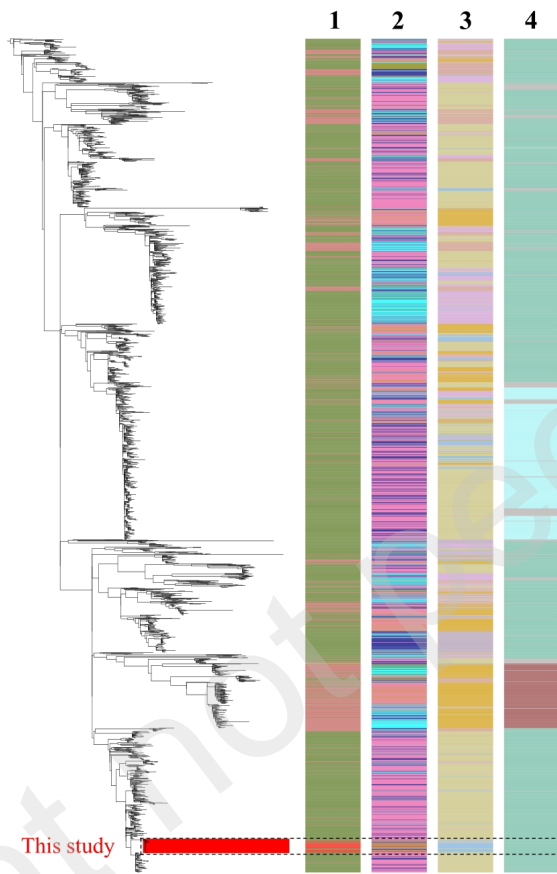
- Pre\_1990s
- 1991-1995
- 1996-2000
- 2001-2005
- 2006-2010
- 2011-2015
- 2016-2020
- 2021
- 2022

3 Place\_of\_Isolation

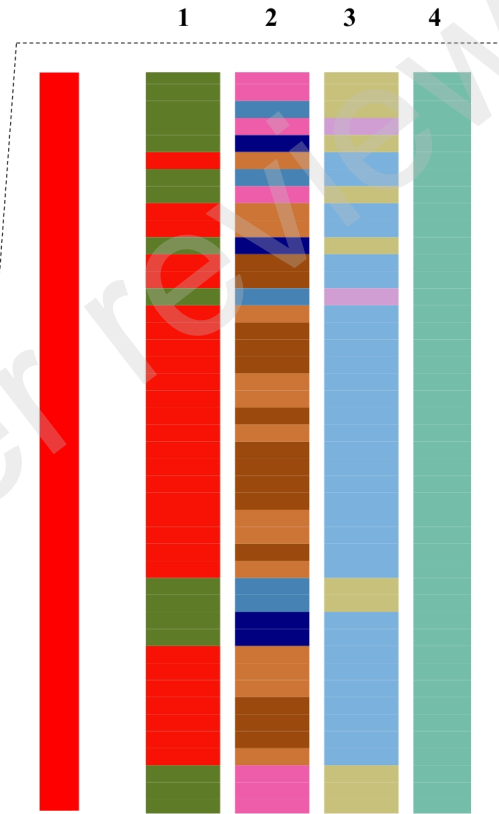
- Asia
- Africa
- Europe
- North America
- South America
- Oceania

4 MLST\_STs

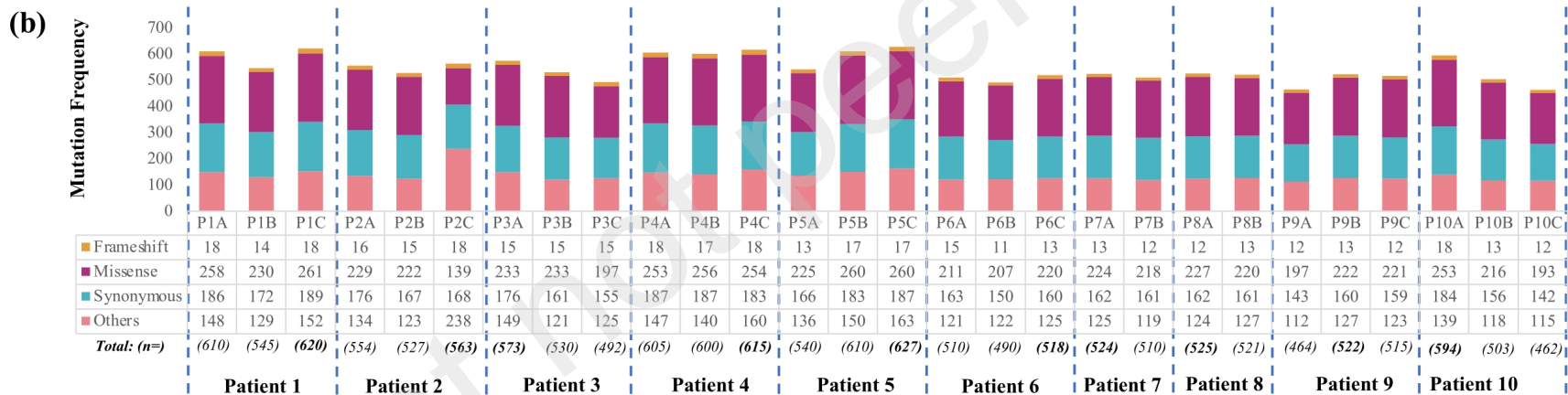
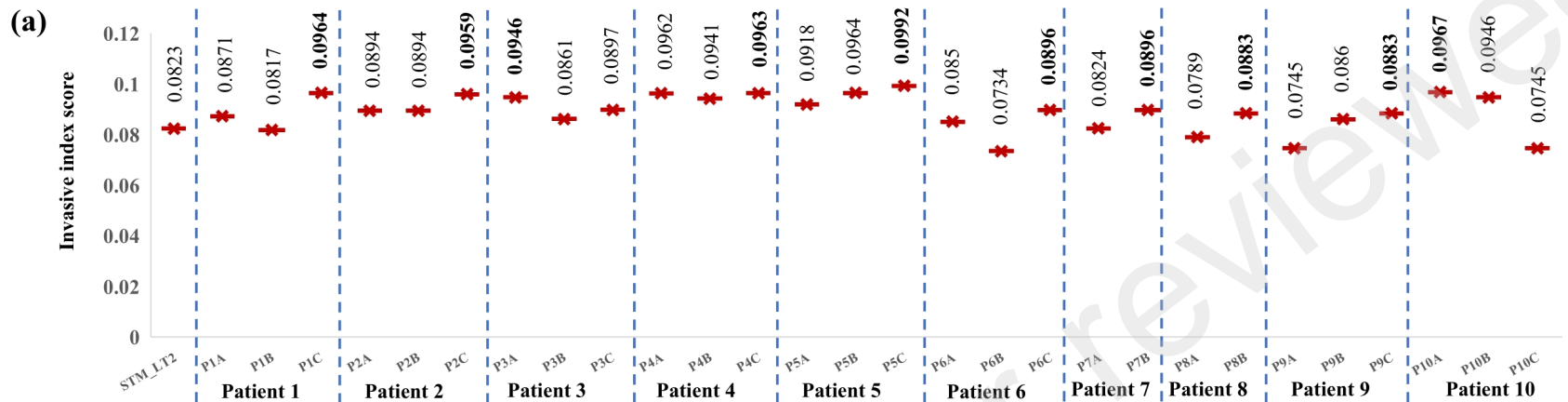
- ST19
- ST34
- ST313
- Others

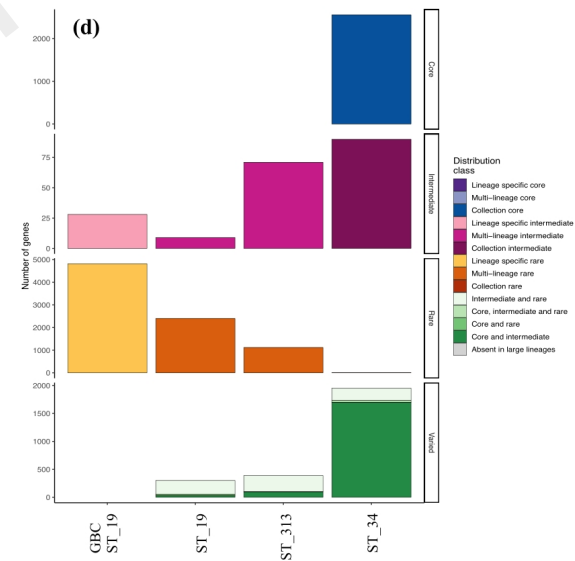
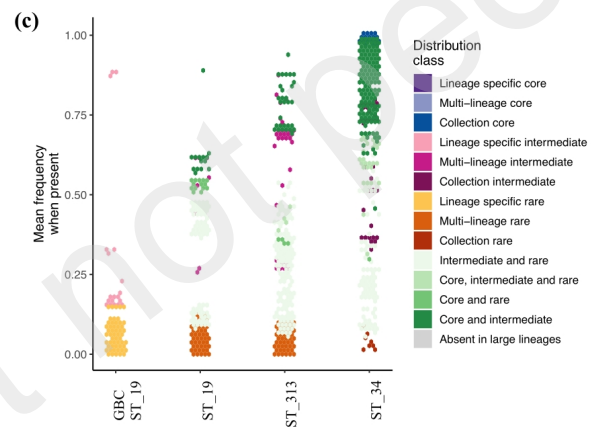
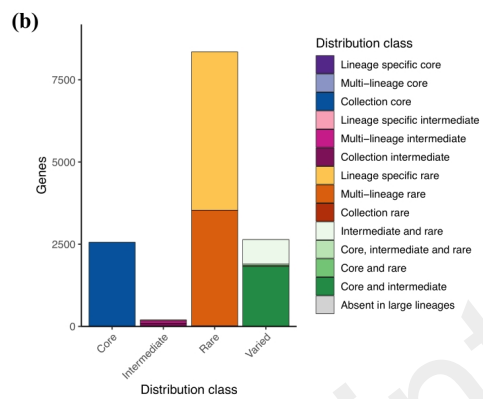
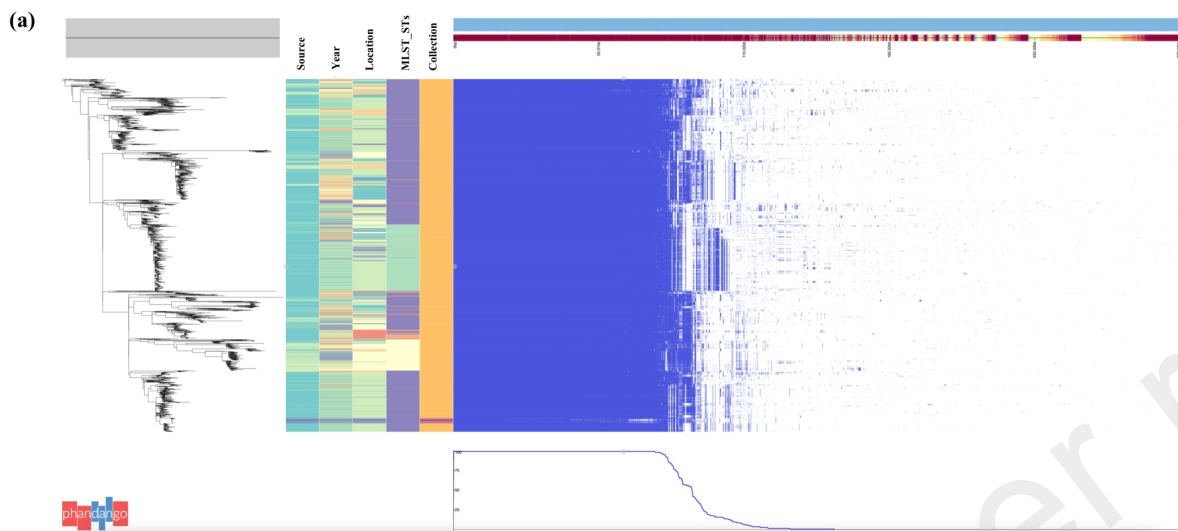


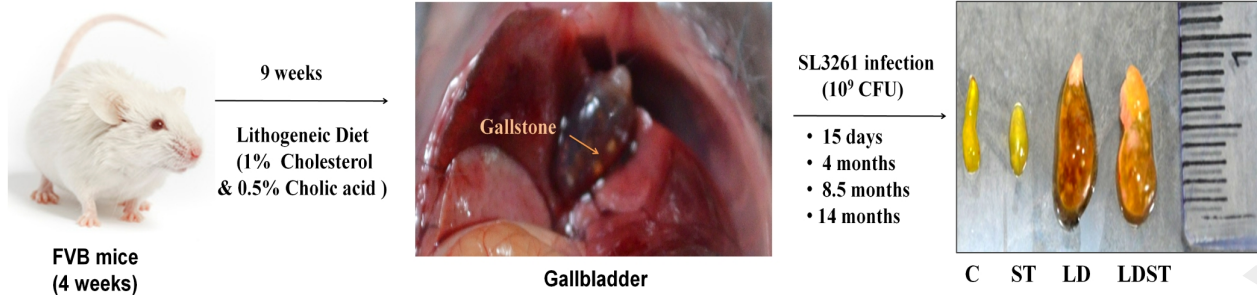
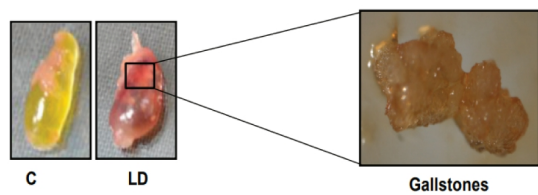
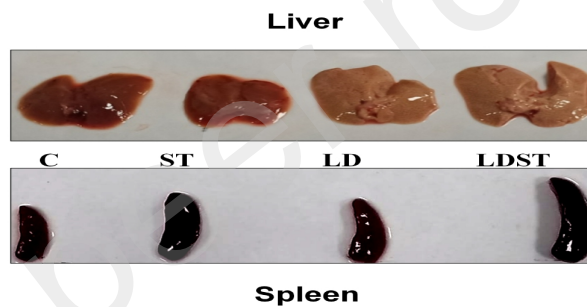
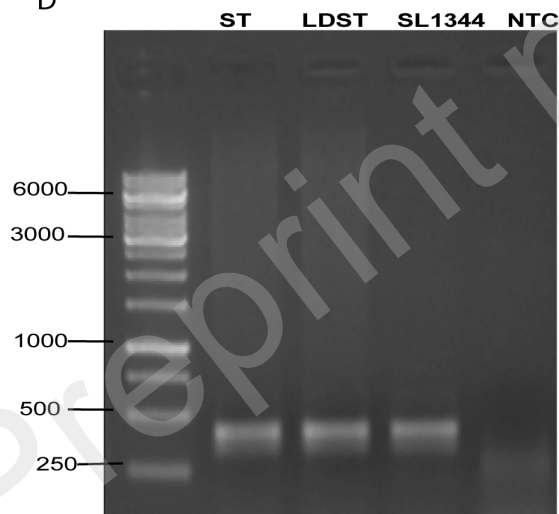
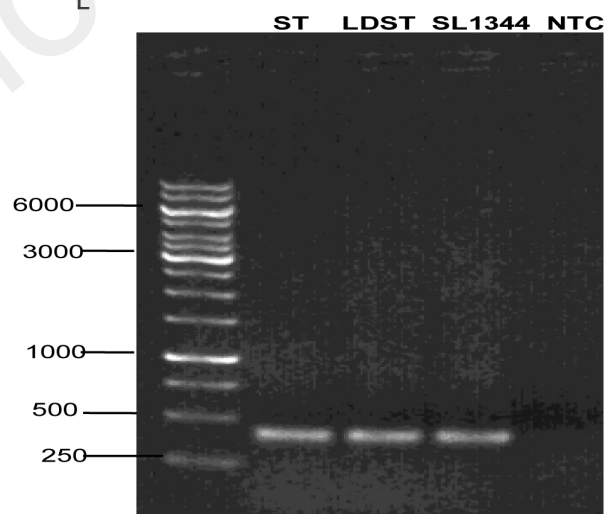
(b)

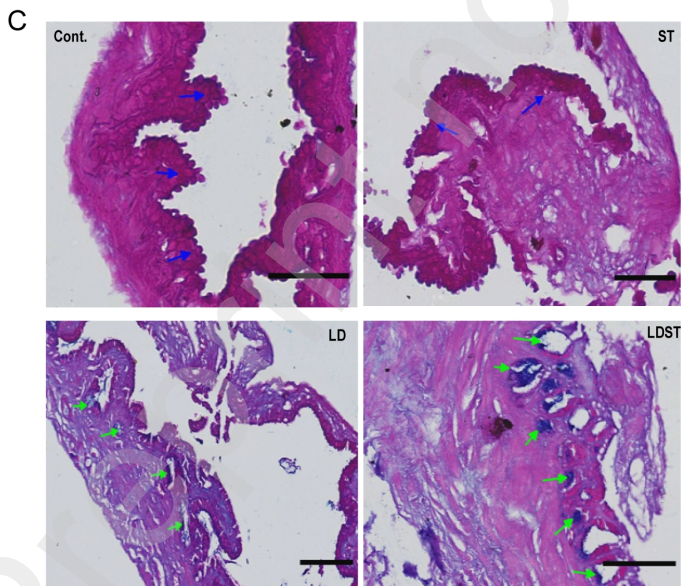
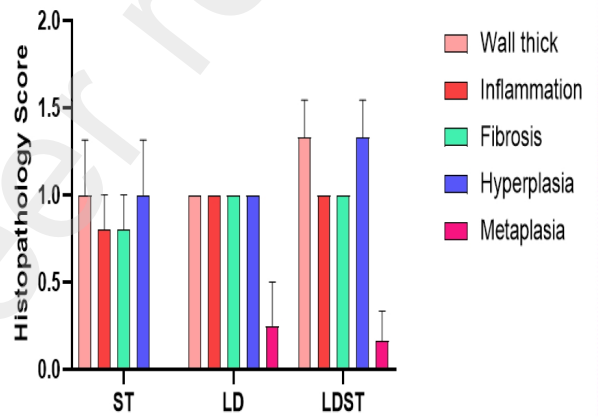
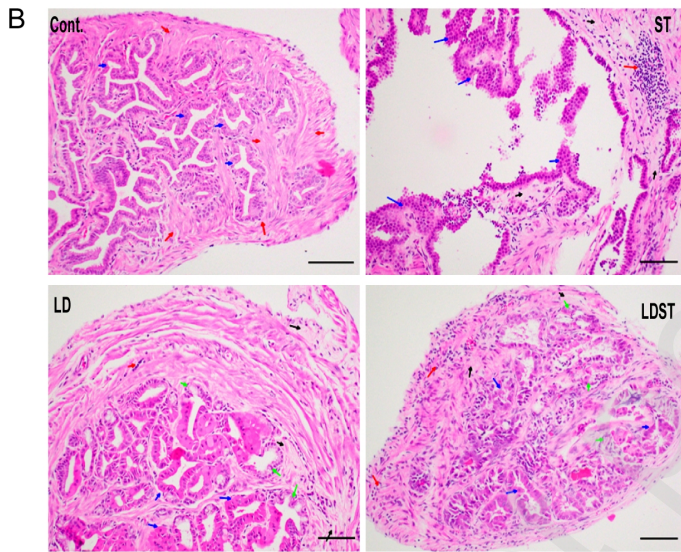
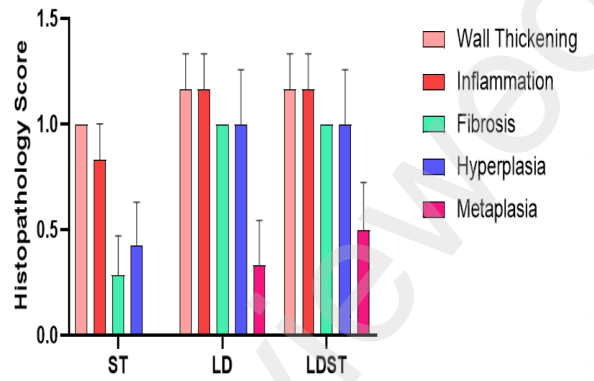
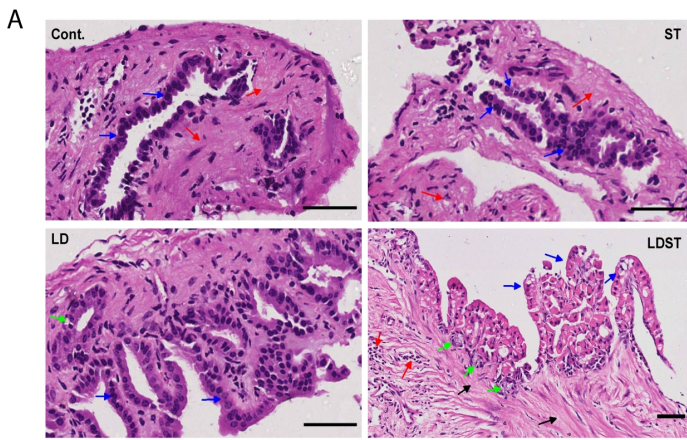


Preprint not certified by peer review

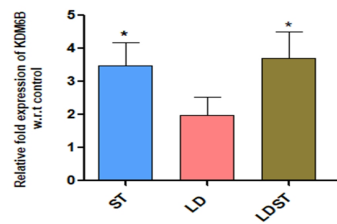




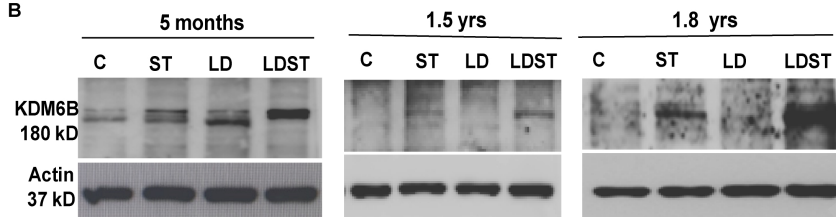
**A****B****C****D****E**



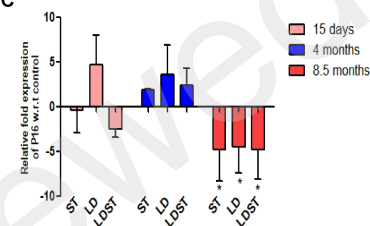
A



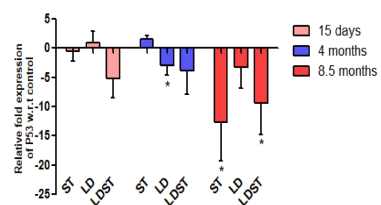
B



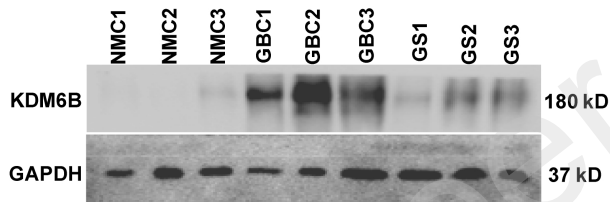
C



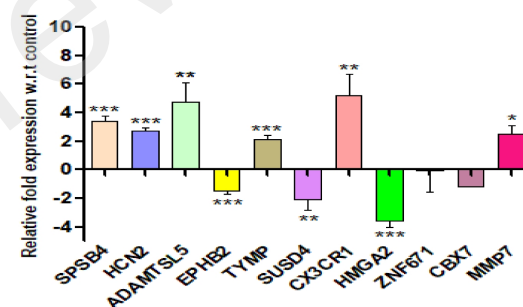
D



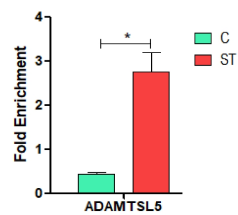
E



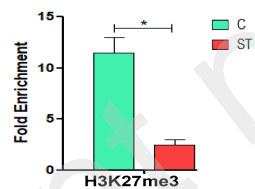
F



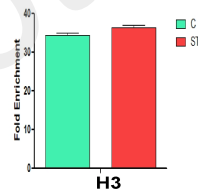
G



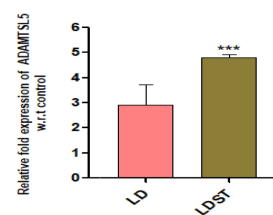
H



I

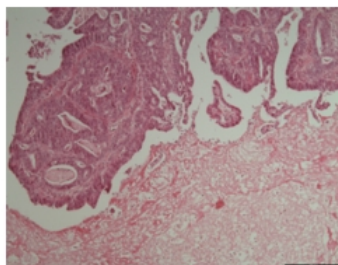


J

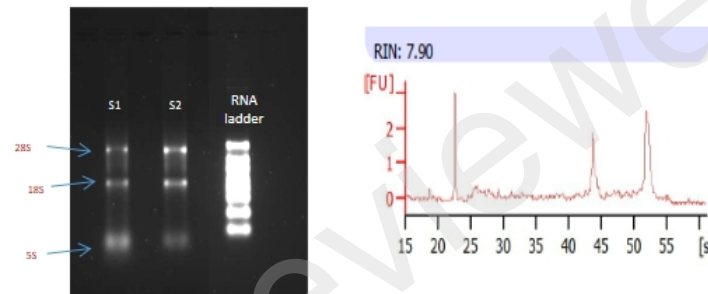




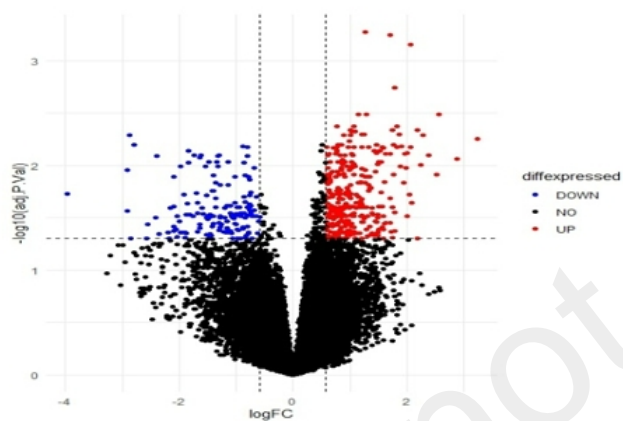
(a)



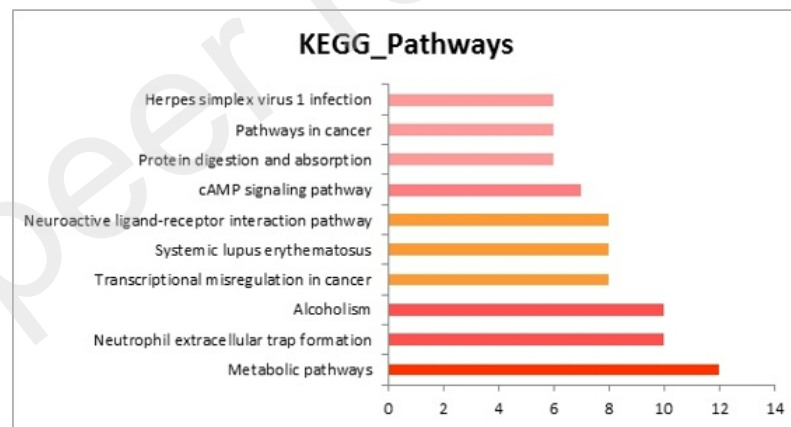
(b)



(c)



(d)



(e)

Preprint not peer reviewed



## Tables

**Table 1:** 16S rRNA raw reads processing information of the faecal samples from GBS (n=20) and GBC (n=20) patients

Sample name	Classification	No of raw reads	No of qualified reads	Average read length
SO 9130 1	GBS (Gall bladder stone)	51766	50945	1352.6
SO 9130 11		58224	57680	1353.6
SO 9130 12		55014	53974	1196
SO 9130 16		62999	61195	1306.7
SO 9130 17		44113	38105	1220.5
SO 9130 18		35924	35580	1278.4
SO 9130 2		74288	72889	1297.2
SO 9130 21		28241	27862	1281.1
SO 9130 23		33965	33717	1350.4
SO 9130 29		41458	41077	1341.8
SO 9130 3		29574	29247	1336.3
SO 9130 31		36022	35488	1290.2
SO 9130 32		32977	32281	1264.5
SO 9130 36		55846	55453	1350.3
SO 9130 37		36446	36135	1349.3
SO 9130 39		30600	30378	1352.1
SO 9130 4		57760	57241	1327.3
SO 9130 40		22899	22719	1330.7
SO 9130 5		41918	41444	1307.5
SO 9130 8		54128	53011	1297.5
SO 9130 10	GBC (Gall bladder cancer)	57272	56042	1224.2
SO 9130 13		36056	35211	1289.1
SO 9130 14		45718	44339	1289.4
SO 9130 15		77590	70719	972.2
SO 9130 19		44073	33802	1328.8
SO 9130 20		58939	58450	1328.8
SO 9130 22		35302	35024	1348.8
SO 9130 24		24749	24525	1347.6
SO 9130 25		36856	36397	1315.5
SO 9130 26		37002	36772	1366.5
SO 9130 27		28958	28719	1366.5
SO 9130 28		29215	28909	1307.6
SO 9130 30		42628	42149	1306.6
SO 9130 33		47905	47512	1306.6
SO 9130 34		28864	28648	1306.6
SO 9130 35		50459	50052	1360.2
SO 9130 38		43271	42937	1340.4
SO 9130 6		58345	57660	1344.3
SO 9130 7		39786	39021	1344.3
SO 9130 9		55193	54430	1309.4

**Table 2:** Preprocessing and quality assessment of 16S rRNA raw reads of tissue sample from GBC patients (n=9)

Patient ID	Input Read pairs	Both surviving reads	%Both Surviving Read	Forward Only Surviving Reads	%Forward Only Surviving Read	Reverse Only Surviving Reads	%Reverse Only Surviving Read	Dropped Reads	%Dropped Read	Merged reads	%merged read
P3C	276970	200064	72.23	15235	5.5	50200	18.12	11471	4.14	53228	26.6054862
P4A	291159	214779	73.77	16669	5.73	48123	16.53	11588	3.98	64811	30.17566894
P4B	278842	206969	74.22	15756	5.65	45194	16.21	10923	3.92	67637	32.6797733
P4C	290395	219426	75.56	15079	5.19	46573	16.04	9317	3.21	74824	34.09987877
P5A	261265	191532	73.31	14881	5.7	44222	16.93	10630	4.07	54024	28.20625274
P5B	307164	226657	73.79	17132	5.58	51066	16.62	12309	4.01	70844	31.25603886
P5C	273855	202276	73.86	16295	5.95	44578	16.28	10706	3.91	59336	29.33417707
P6A	325482	247558	76.06	17772	5.46	50613	15.55	9539	2.93	83576	33.76016933
P6B	260129	199496	76.69	14381	5.3	39018	15	7234	2.78	66430	33.29891326

**Table 3:** Multi locus sequence typing (MLST) allelic profile of the study isolates depicting sequence types (STs) based on seven housekeeping genes

	<i>IDs</i>	<i>ST</i>	<i>aroC</i>	<i>dnaN</i>	<i>hemD</i>	<i>hisD</i>	<i>purE</i>	<i>sucA</i>	<i>thrA</i>
Patient 1	P1A	19	10	7	12	9	5	9	2
	P1B	19	10	7	12	9	5	9	2
	P1C	19	10	7	12	9	5	9	2
Patient 2	P2A	19	10	7	12	9	5	9	2
	P2B	19	10	7	12	9	5	9	2
	P2C	19	10	7	12	9	5	9	2
Patient 3	P3A	19	10	7	12	9	5	9	2
	P3B	ND	ND	7	12	9	5	9	2
	P3C	19	10	7	12	9	5	9	2
Patient 4	P4A	19	10	7	12	9	5	9	2
	P4B	19	10	7	12	9	5	9	2
	P4C	19	10	7	12	9	5	9	2
Patient 5	P5A	19	10	7	12	9	5	9	2
	P5B	ND	~10	7	12	9	5	9	2
	P5C	19	10	7	12	9	5	9	2
Patient 6	P6A	19	10	7	12	9	5	9	2
	P6B	ND	10	7	12	9	ND	ND	2
	P6C	19	10	7	12	9	5	9	2
Patient 7	P7A	19	10	7	12	9	5	9	2
	P7B	19	10	7	12	9	5	9	2
Patient 8	P8A	19	10	7	12	9	5	9	2
	P8B	19	10	7	12	9	5	9	2
Patient 9	P9A	ND	10	7	12	9	ND	ND	2
	P9B	19	10	7	12	9	5	9	2

	P9C	19	10	7	12	9	5	9	2
Patient 10	P10A	19	10	7	12	9	5	9	2
	P10B	19	10	7	12	9	5	9	2
	P10C	ND	10	7	12	9	ND	ND	2

ND- Not determined

**Table 4:** Detection of plasmid and plasmid replicons in the studied genome of *S. Typhimurium*, ST- 19 isolated from GBC (n=28) with reference to *S. Typhimurium* LT2 (ST-19 serovar) as identified by PLSDB and REBASE

		plasmid P02	plasmid pSE81-1705-3	plasmid 3	CFSAN002003 plasmid (100% identity with pSLT)
GC content		52.6%	50.2%	52.2%	53.1%
Virulence gene		<i>entD</i>	<i>galU</i>	<i>entD</i>	<i>pefC, spvB, spvC, pefD, rck, pefA, pefB</i>
Plasmid replicons		NA	NA	NA	<i>IncFII, IncFI</i>
Patient 1	P1A	+	+	+	-
	P1B	+	+	+	-
	P1C	+	+	-	-
Patient 2	P2A	+	+	-	-
	P2B	+	+	-	-
	P2C	+	+	+	+
Patient 3	P3A	+	+	+	+
	P3B	+	+	-	-

	P3C	+	-	+	-
Patient 4	P4A	+	+	+	-
	P4B	+	+	-	-
	P4C	+	+	-	-
Patient 5	P5A	+	+	-	+
	P5B	+	+	-	+
	P5C	+	+	-	+
Patient 6	P6A	+	+	-	+
	P6B	+	+	-	+
	P6C	+	+	+	-
Patient 7	P7A	+	+	+	-
	P7B	+	+	+	-
Patient 8	P8A	+	+	+	-
	P8B	+	+	+	+

Patient 9	P9A	+	+	+	+
	P9B	+	+	+	+
	P9C	+	+	+	+
Patient 10	P10A	+	+	+	-
	P10B	+	+	+	-
	P10C	+	+	+	-

+ indicates present, - indicates absent

**Table 5:** Detection of prophage and prophage remnants in the studied genome of *S. Typhimurium*, ST- 19 isolated from GBC (n=28) with reference to invasive D23580 African isolate (ST-313)

	Gifsy-1	Gifsy-2	Salmon_118970_Sal3	Def-1	Def-2	Def-3	Def-4	ST64B
D23580 (ST313)	+	+	Not determined	+	+	+	+	+
P1A	+	+	*	+	+	+	+	+
P1B	+	+	*	+	+	+	+	+
P1C	+	+	*	+	+	+	+	+
P2A	+	+	*	+	+	+	+	+
P2B	+	*	*	+	+	+	-	+
P2C	+	*	*	+	+	+	+	+
P3A	+	+	*	+	+	+	+	+
P3B	+	+	*	+	+	*	-	+
P3C	+	+	*	+	+	*	+	+
P4A	+	+	*	+	+	+	+	+
P4B	+	+	*	+	+	+	+	+
P4C	+	+	*	+	+	+	+	+
P5A	+	*	*	+	+	+	+	+
P5B	+	+	*	+	+	+	+	+
P5C	+	+	*	+	+	+	-	+
P6A	+	*	*	+	+	+	-	+
P6B	+	+	*	*	+	+	+	+

P7A	+	+	*	+	+	+	+	+
P7B	+	*	*	+	+	+	+	+
P8A	+	*	*	+	+	+	+	+
P8B	+	*	*	+	+	+	+	+
P9A	+	+	*	*	+	+	+	+
P9B	+	*	*	+	+	+	+	+
P9C	+	*	*	+	+	+	+	+
P10A	+	+	*	+	+	+	+	+
P10B	+	+	*	+	+	+	+	+
P10C	+	+	*	*	+	+	+	+
P6C	+	+	*	+	+	+	+	+

*S. Typhimurium* D23580- ST313 (invasive African strain), + = present, - = absent, \* = Query coverage below < 35%. Gifsy-1, Gifsy-2 and **Salmon\_118970\_Sal3 phages** were detected by PHASTER